PNL-6790
UC-510

Processing Summary Report: Fabrication of Cesium and Strontium Heat and Radiation Sources

L. K. Holton, Jr.
J. E. Surma
R. P. Allen
R. A. Brouns
G. H. Bryan
M. L. Elliott
R. W. Goles
F. E. Haun
R. F. Klein
R. D. Peters

February 1989

Prepared for the U.S. Department of Energy
under Contract DE-AC06-76RLO 1830

Pacific Northwest Laboratory
Operated for the U.S. Department of Energy
by Battelle Memorial Institute

Battelle

PNL-6790

DISCLAIMER

PACIFIC NORTHWEST LABORATORY
operated by
BATTELLE MEMORIAL INSTITUTE
for the
UNITED STATES DEPARTMENT OF ENERGY
under Contract DE-AC06-76RLO 1830

Printed in the United States of America
Available from
National Technical Information Service
United States Department of Commerce
5285 Port Royal Road
Springfield, Virginia 22161

NTIS Price Codes
Microfiche A01

Printed Copy

Pages	Price Codes
001-025	A02
026-050	A03
051-075	A04
076-100	A05
101-125	A06
126-150	A07
151-175	A08
176-200	A09
201-225	A10
226-250	A11
251-275	A12
276-300	A13

8/88

DISCLAIMER

PNL-6790
UC-510

PNL--6790

DE89 008314

PROCESSING SUMMARY REPORT: FABRICATION OF CESIUM AND STRONTIUM HEAT AND RADIATION SOURCES

L. K. Holton, Jr.,
J. E. Surma
R. P. Allen
R. A. Brouns
G. H. Bryan
M. L. Elliott
R. W. Goles
F. E. Haun
R. F. Klein
R. D. Peters

February 1989

Prepared for
the U.S. Department of Energy
under Contract DE-AC06-76RLO 1830

Pacific Northwest Laboratory
Richland, Washington 99352

PROCESSING SUMMARY REPORT: FABRICATION OF CESIUM AND STRONTIUM HEAT AND RADIATION SOURCES

SUMMARY

The Pacific Northwest Laboratory (PNL)[(a)], under contract to the U.S. Department of Energy, has produced 30 isotopic heat sources (canisters) for the Federal Republic of Germany (FRG) to be used as part of a repository testing program in the Asse Salt Mine. PNL program work involved the filling, closure, and decontamination of the 30 canisters. The canisters were fabricated (filled) in three separate processing campaigns using the radioactive liquid-fed ceramic melter to produce a borosilicate glass. Within the borosilicate glass matrix radiochemical constituents (^{137}Cs and ^{90}Sr) were immobilized to yield a product with a predetermined decay heat and surface radiation exposure rate. The average radiochemical characteristics of each set of ten canisters are summarized below:

Number of Canisters	Average ^{137}Cs Content, kCi	Average ^{90}Sr Content, kCi	Estimated Decay Heat, W	Estimated Surface Exposure, R/hr
10	192	85	1490	272,000
10	78	143	1330	112,000
10	207	130	1860	310,000

The canisters were lid-welded using an autogenous gas tungsten arc (GTA) welding process. Leak tightness of the canister lid weld was verified by a helium leak test to be no greater than 2.4×10^{-8} atm-cc/sec, which was less than the leak rate criterion of 10^{-7} atm-cc/sec.

The top, sides, and bottom of the canisters were decontaminated by electropolishing technology. All canisters were decontaminated to surface

---

(a) PNL is operated for the U.S. Department of Energy (DOE) by Battelle Memorial Institute under Contract DE-AC06-76RLO 1830.

smear contamination levels that were less than 33 Bq/100 cm^2 beta-gamma radiation. No significant alpha contamination was observed on the surfaces of the canister. The canisters were characterized in a series of five tests: 1) surface temperature measurement, 2) surface exposure rate, 3) gamma energy scanning, 4) canister mass determination, and 5) gauge testing. The surface temperatures of the canisters ranged from a minimum average temperature of 133°C to a maximum average temperature of 205°C. All but eight of the canisters had surface exposure rates in the range of 218,000 to 320,000 R/hr. Results from the gamma energy scanning of the canisters correlated well with previous knowledge of the radiochemical characteristics of the canisters. The average glass mass in the canister was 158 kg and the average canister fill volume was 60.6 liters. All canisters passed easily through the ovality gauge (306-mm inside diameter).

ACKNOWLEDGMENTS

A project as large and challenging as the fabrication of the heat and radiation sources for the Federal Republic of Germany necessarily required the technical skills of many people. This technical support was provided by engineers and technicians primarily from the Process Application Section of PNL's Process Technology Department under the supervision of H. C. Burkholder.

The authors gratefully acknowledge the contributions to the canister filling operations by D. L. Alexander, G. N. Buck, E. L. Doan, J. L. Duce, J. E. Gose, F. A. Graf, C. W. Hall, S. D. Halstead, J. S. Hammack, J. F. Hutchens, D. O. Jenkins, and S. J. Morris and the technical support provided in welder operations by D. O. Jenkins and D. L. Alexander; in canister helium leak checking and canister characterization operations by J. L. Duce, J. F. Hutchens, and G. N. Buck; and in canister decontamination by electropolishing and canister characterization operation by S. D. Halstead and S. J. Morris.

CONTENTS

Contents (cont'd)

FIGURES

Figures (cont'd)

TABLES

1.0 INTRODUCTION

Thirty isotopic heat and radiation sources (canisters) were produced using a remotely operated radioactive liquid-fed ceramic melter (RLFCM). These sources contain highly radioactive species and are to be used as part of a repository testing program in the Asse Salt Mine located in northeastern West Germany. The canisters were closed using a remotely operated welding system and were then decontaminated utilizing an electropolishing process. Physical characteristics of the canisters were measured using a series of nondestructive tests and measurements.

The canisters were filled with a borosilicate glass in PNL's radiochemical engineering cell complex in the 324 Building, where the RLFCM, along with associated supporting equipment, was located in the largest of four hot cells. This equipment included the feed makeup and feed system, the canister handling and storage systems, and the off-gas treatment system of the RLFCM. Lids were welded on the canisters after all thirty had been filled.

After the welding of the canister lid to the canister, it was passed into an air lock between the hot cell containing the vitrification equipment and the cell containing the decontamination equipment. In the air lock the integrity of the lid weld was verified using a helium leak-detection system and the canister surface exposure rate was measured.

The surfaces of the canisters were decontaminated using an electropolishing process. The remaining physical measurements were performed in the decontamination cell before the canisters were placed in a water-cooled storage rack, where they will remain until their shipment to the FRG.

2.0 CANISTER FILLING

The FRG canisters were filled with radioactive borosilicate glass using the radioactive liquid-fed ceramic melter process located in B-Cell of the 324 Building (Figure 2.1). A schematic of the FRG canister filling process is depicted in Figure 2.2. Canisters were filled in three successive campaigns (RLFCM-7, -8, and -9) of ten canisters each. Radioactive feed slurries, prepared by blending ^{137}Cs and ^{90}Sr concentrates and glass-forming chemicals in the waste preparation equipment, were fed from a feed makeup tank to the RLFCM using a slurry metering system. In the RLFCM, the liquid waste was calcined and melted to form a borosilicate glass. Glass temperatures within the RLFCM were maintained at 1100 to 1200°C during waste feeding operations and at 1050°C during idling periods between waste feeding operations. The molten glass product formed in the RLFCM was then airlifted in approximately 20-L batches into stainless steel canisters positioned by a rotating turntable below the melter discharge trough. The glass level in the canister being filled was remotely monitored by a gamma-level detection system. Once filled, the canister was removed from the turntable, a dust cover placed on the canister, and placed in an insulated cooling pod. After cooling, the canister was transferred to another part of the cell, where it was stored for ~1 yr until the sealing and decontamination processing steps could be completed.

Radiochemical characteristics of the three sets of ten canisters are presented in Table 2.1. Production of the glass canisters required that specified amounts of ^{137}Cs and ^{90}Sr be mixed into the feed slurry. The melter glass was brought into specification with respect to cesium and strontium before glass was poured into the first production canister (canister #1). The average compositions for the FRG glass in each of the three production campaigns are summarized in Table 2.2. The estimated chemical composition of each of the 30 canisters is summarized in Appendix A.

Typically there were three glass pours into each canister during filling. For most of the canisters, glass samples were obtained from two of the three pours. The samples were analyzed for all chemical constituents through inductively coupled plasma emission spectroscopy analysis (ICP).

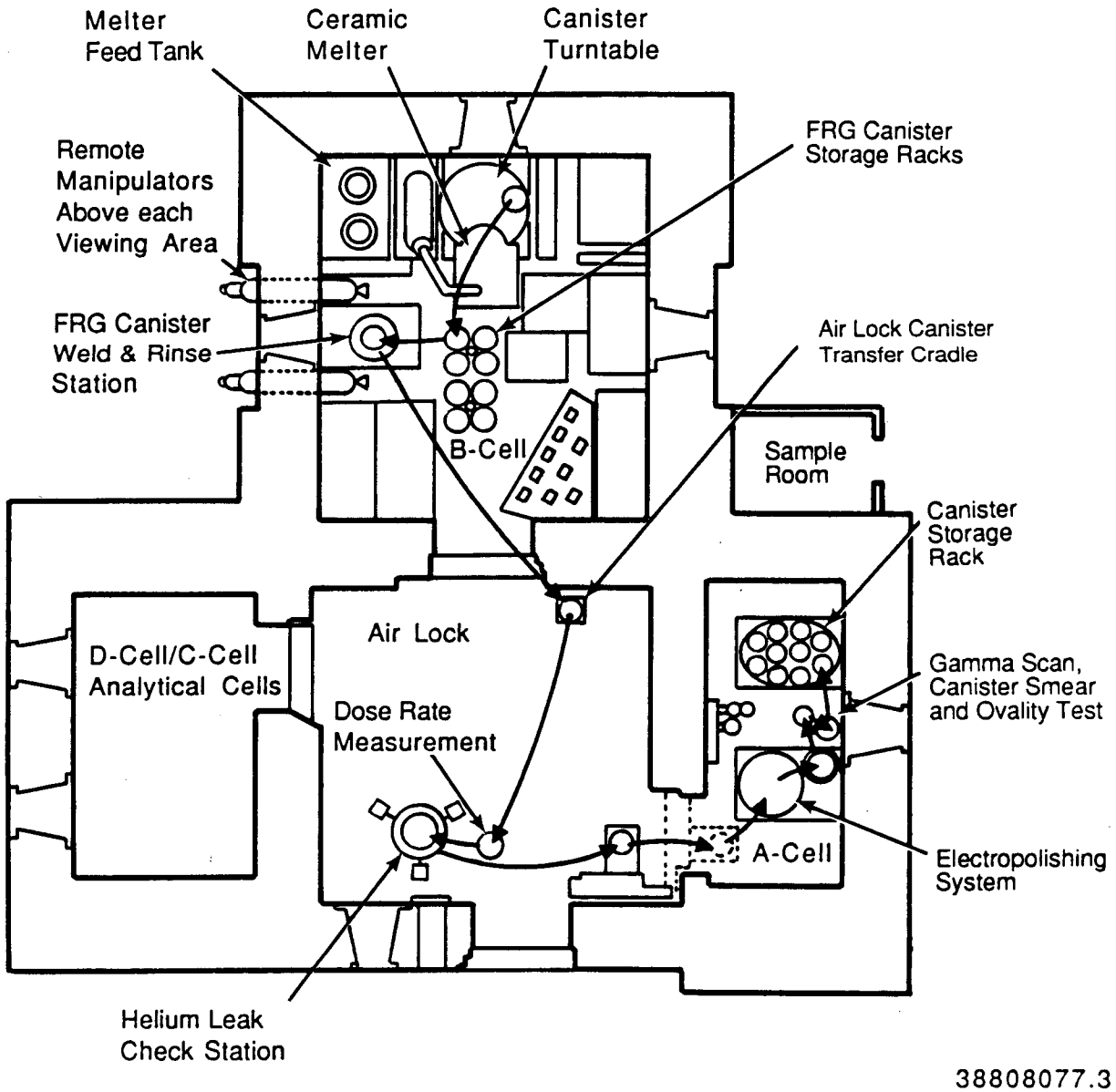

FIGURE 2.1. Plan View of the Radiochemical Engineering Cell Complex Showing Locations for Processing of the FRG Canisters

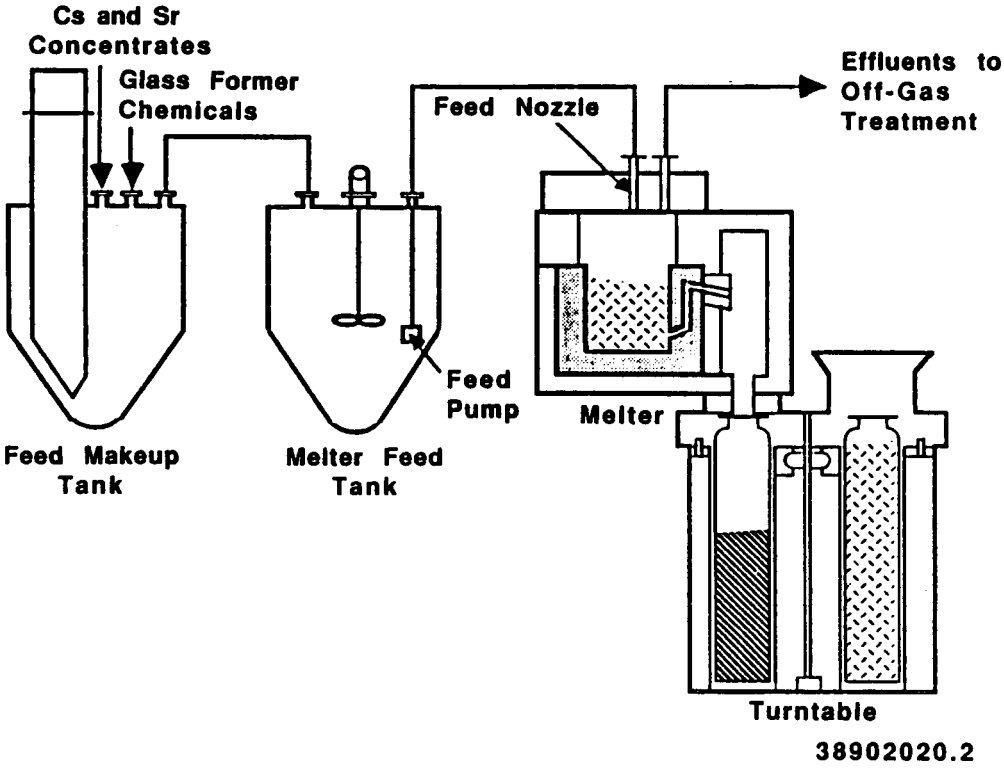

FIGURE 2.2. FRG Canister Filling Process

TABLE 2.1. Average Radiochemical Characteristics of the FRG Canisters

Campaign	Average ^{137}Cs Content/Canister, kCi	Average ^{90}Sr Content/Canister, kCi	Average Decay Heat/Canister, watts	Average Surface Exposure Rate, R/hr
RLFCM-7	192	85	1490	272,000
RLFCM-8	78	143	1330	112,000
RLFCM-9	207	130	1860	310,000

Cesium-137 analysis was completed by gamma spectrometry, and ^{90}Sr analysis was completed by cation exchange separation and beta counting. These analytical methods are described in Appendix B. The weighted average composition for each canister, summarized in Appendix A, was determined using the individual glass sample analyses and weighting the analysis results by the mass of the pour from which the sample was obtained. Figure 2.3 presents the concentrations of the major glass components for the first set of ten canisters. It is seen from the plot that the concentrations of silicon dioxide and sodium oxide are variant for the first five or six canisters produced. This

TABLE 2.2. Nominal Glass Compositions of the FRG Canisters

Oxide Compound	Average Glass Composition RLFCM-7, wt%	Average Glass Composition RLFCM-8, wt%	Average Glass Composition RLFCM-9, wt%
Al_2O_3	2.88	2.58	2.17
B_2O_3	13.68	14.65	14.84
BaO	1.05	1.13	1.02
CaO	1.52	1.25	0.79
CeO_2	0.06	0.05	0.07
Cr_2O_3	0.58	0.38	0.45
Cs_2O	5.02	2.08	5.74
Fe_2O_3	11.18	10.10	9.93
La_2O_3	1.04	1.07	1.53
Li_2O	0.31	0.00	0.00
MgO	0.78	0.54	0.44
MnO_2	0.80	1.20	1.11
MoO_3	0.05	0.00	0.00
Na_2O	16.50	13.22	11.58
Nd_2O_3	0.65	0.71	0.89
NiO	0.39	0.25	0.44
PbO	0.16	0.00	0.00
RuO_2	0.02	0.00	0.00
SiO_2	41.25	48.02	46.59
SrO	1.65	2.67	2.34
TiO_2	0.19	0.07	0.03
ZnO	0.08	0.01	0.00
ZrO_2	0.15	0.04	0.05
	100.00	100.00	100.00

resulted from the unknown presence of high concentrations of sodium in the incoming waste portion of the RLFCM feed. When the glass was analyzed and the higher than normal level of sodium was observed on the analytical results, the feed was corrected by lowering the sodium concentration in the chemical additives to the radioactive feed fraction. The high-sodium

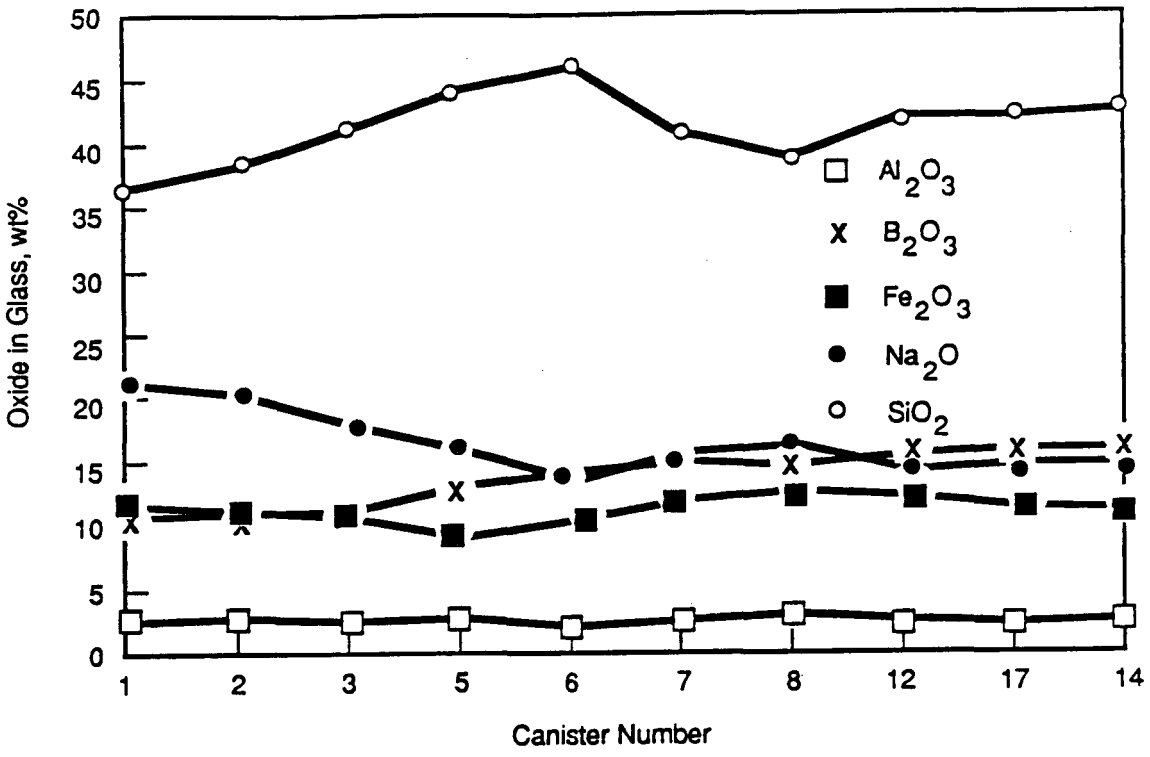

FIGURE 2.3. RLFCM-7 Major Glass Component Concentrations

glass exhibited a lower viscosity than was acceptable for proper operation of the melter; therefore the silicon dioxide level was increased for production of the next three canisters. The composition of the glass was stabilized by the time the sixth canister was produced and remained fairly constant throughout the remainder of the campaign.

For the RLFCM-7 canisters the target concentration of cesium oxide and strontium oxide was 5.73 and 1.9 wt%, respectively. Figure 2.4 shows the concentrations for cesium and strontium oxides for these canisters. The strontium oxide concentration was determined directly from the ICP analysis of the glass samples taken during glass pouring. The cesium oxide concentration was determined using the radiochemical analytical results to back-calculate the oxide concentration from the known isotopic abundance of the ^{137}Cs isotope. Radiochemical analysis was also conducted for the ^{90}Sr isotope. It is seen from Figure 2.4 that the concentration of strontium oxide remained fairly constant throughout the ten-canister campaign. The concentration of cesium oxide, however, varied slightly during canister production.

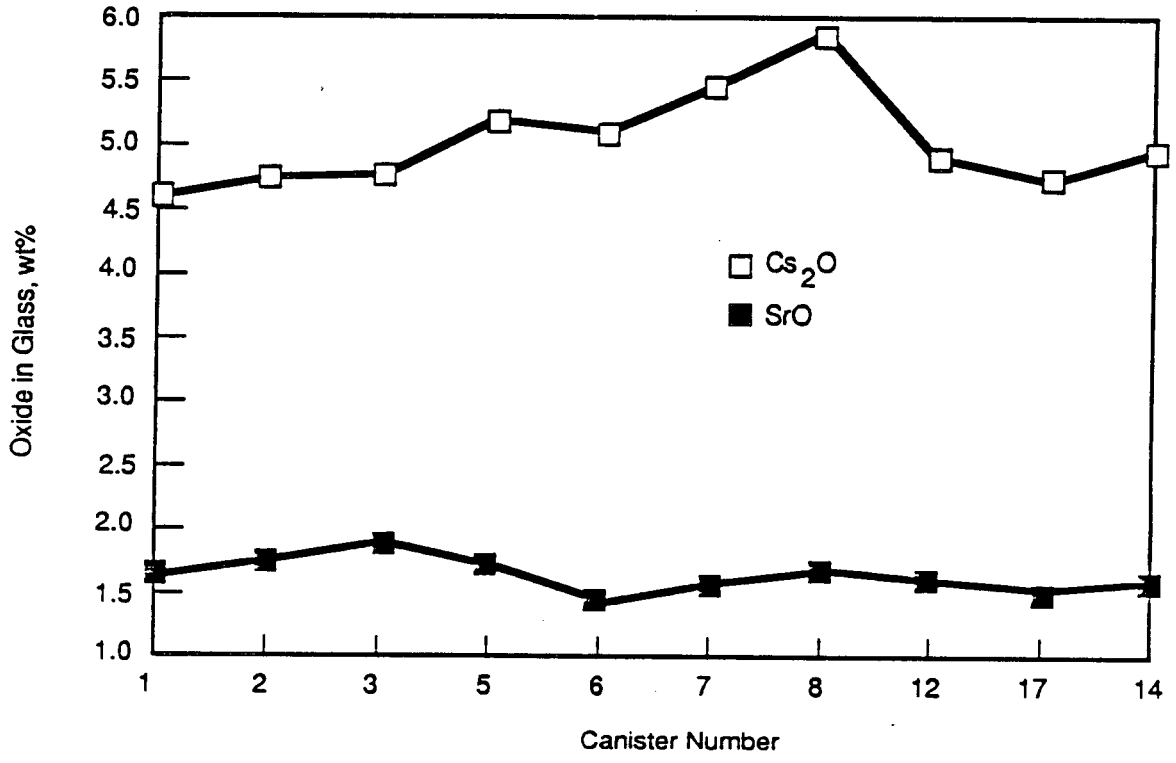

FIGURE 2.4. RLFCM-7 Cesium and Strontium Concentrations

It was observed that variations in the cesium and strontium concentrations were more prevalent than variations in the concentrations of the major glass-forming chemicals. This observance can be attributed primarily to the methods used for feed slurry preparation. Measured amounts of ^{137}Cs and ^{90}Sr concentrates were mixed with appropriate amounts of nonradioactive chemicals in the feed makeup tank. Control of the volume of ^{137}Cs and ^{90}Sr concentrates transferred into the makeup tank was not as reliable as that of the nonradioactive fraction of the feed. The waste fraction contained a very low concentration of solids, and therefore only the cesium and strontium concentrations were affected by volume variations in the waste fraction portion of the feed slurry mixture.

The next set of ten canisters produced (RLFCM-8) were the low-surface-exposure canisters, as indicated in Table 2.1. The concentration of strontium in these canisters was increased and that of cesium was decreased from that of the first set. Shown in Figure 2.5 is the concentration of the cesium and strontium oxides in the glass of the RLFCM-8 canisters. The

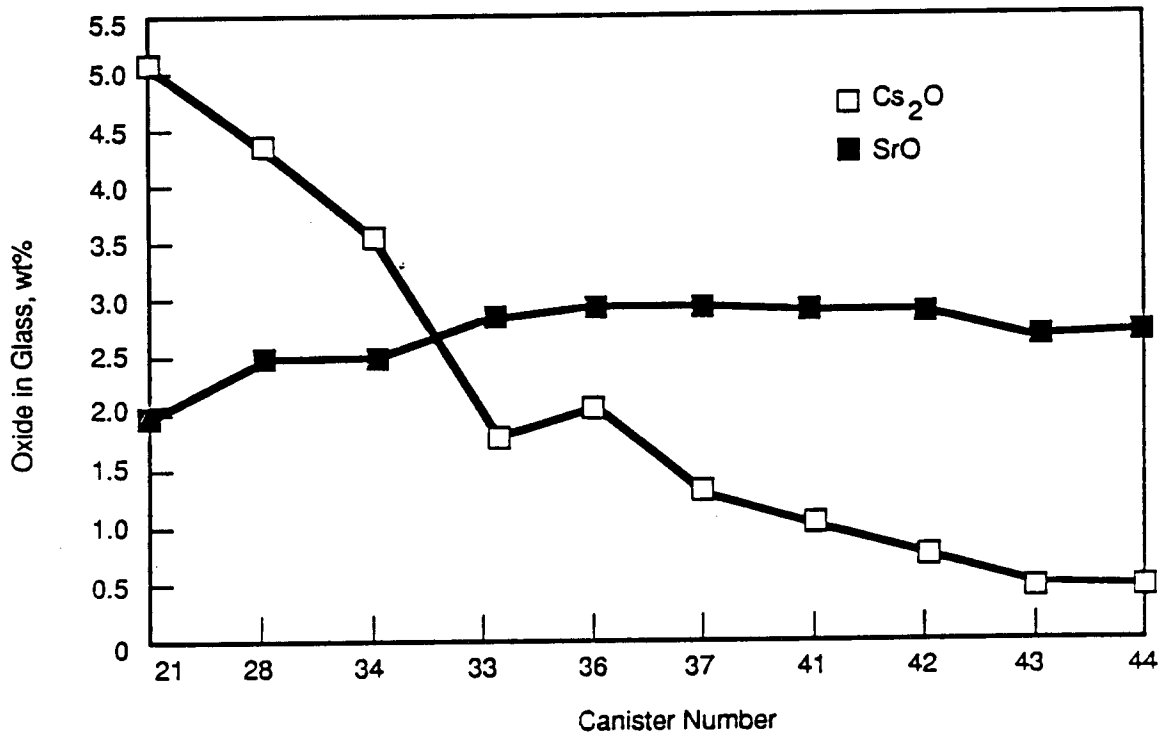

FIGURE 2.5. RLFCM-8 Cesium and Strontium Concentrations

cesium concentration at the onset of this operating campaign was the same as that at the end of the first campaign. No cesium fraction was added to the melter feed slurry; therefore, the concentration of cesium steadily declined throughout the filling of these ten canisters. The objective of this campaign was to produce ten canisters with a constant decay heat of 1680 watts. Because of the high concentration of ^{137}Cs in the RLFCM glass at the onset of this campaign, a feed with high strontium content (i.e., low exposure and high decay heat) was fed to the RLFCM. To maintain a constant decay heat value for all ten canisters, the ^{90}Sr concentration was steadily increased through production of the fifth canister. The ^{90}Sr concentration should have increased at a lesser rate throughout the production of the next five canisters, but due to errors in sample analysis information at the time of feed preparation, strontium concentrations decreased slowly. This resulted in lower than specified decay heat in these last five canisters of RLFCM-8.

Figure 2.6 presents the levels of the major glass constituents for the second set of ten canisters. The plot shows that the concentrations of all

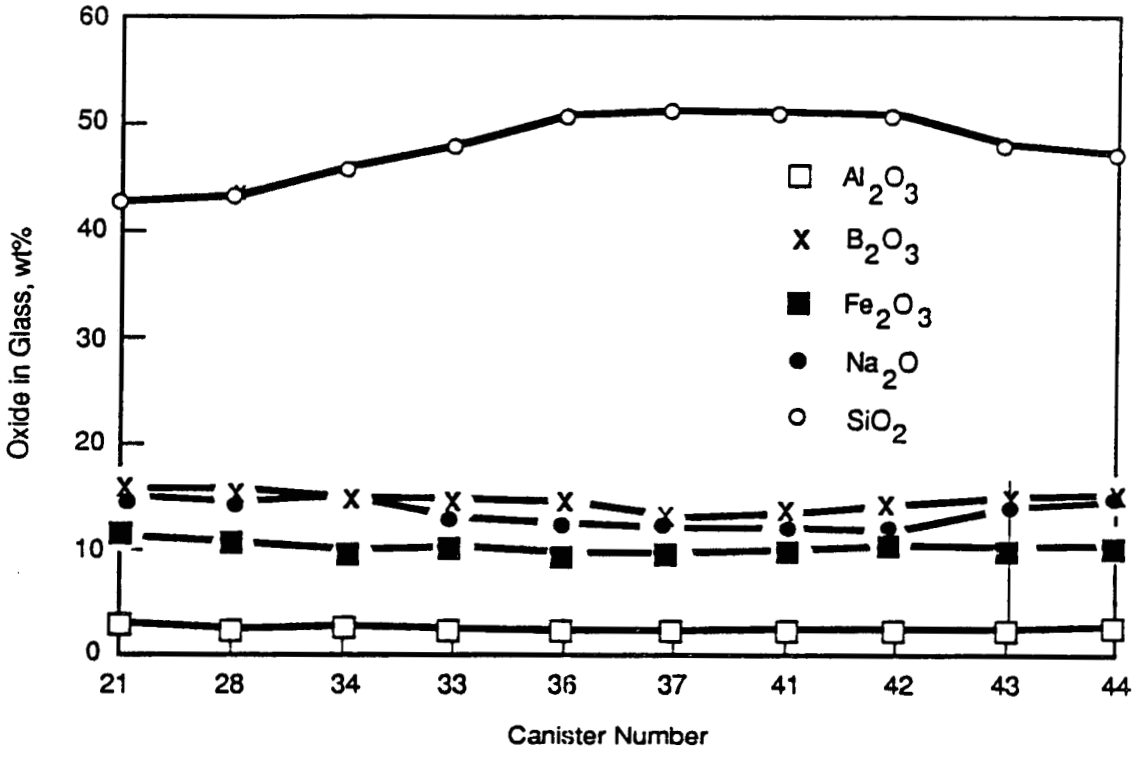

FIGURE 2.6. RLFCM-8 Major Glass Component Concentrations

constituents remained nearly constant throughout production of these canisters.

The third set of ten canisters, as specified, had the highest decay heat and surface exposure rates. From Figure 2.7 it is observed that the concentrations of cesium and strontium oxides in the glass were constant through the production of the fifth canister. Due to inadequate supplies of strontium, cesium was substituted in the glass during the production of the last five of this set of ten canisters. To produce canisters with the decay heat specification of 2 kW/canister, the concentration change of cesium had to increase at a higher rate than the decreasing strontium concentration. This fact is evident from the plots in Figure 2.7.

Presented in Figure 2.8 is the plot of the concentrations of the major glass constituents for the last ten canisters. Very good control of these constituents in the feed formulation was achieved during production of these canisters in RLFCM-9.

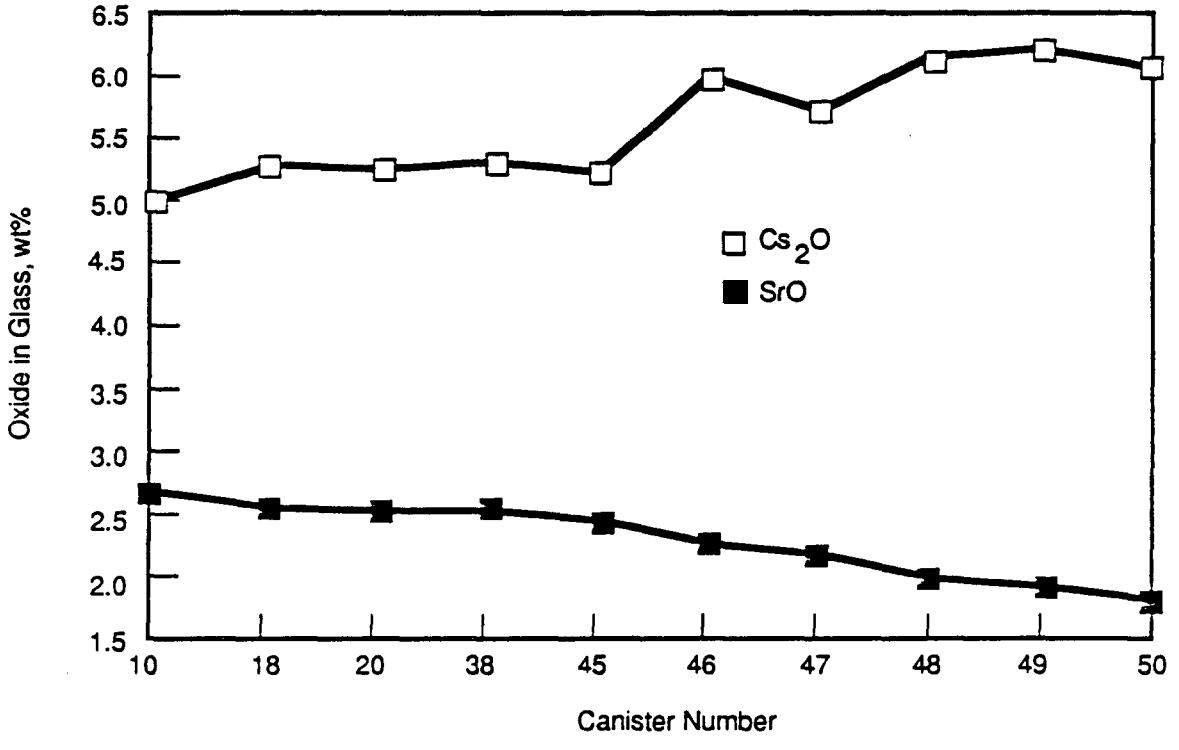

FIGURE 2.7. RLFCM-9 Cesium and Strontium Concentrations

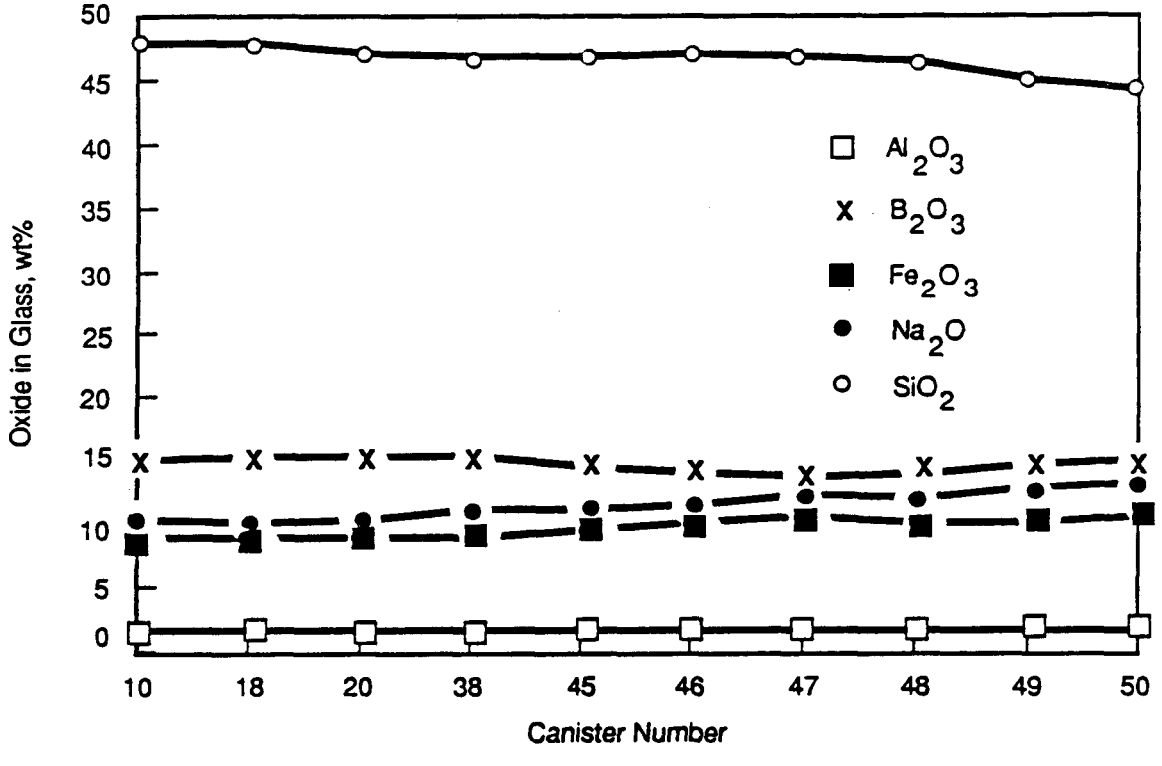

FIGURE 2.8. RLFCM-9 Major Glass Component Concentrations

The concentration of the radiochemical constituents, ^{137}Cs and ^{90}Sr, was used directly to determine the decay heat in each of the 30 canisters. The concentrations of radiochemical constituents in the glass were estimated using the glass sample analysis and glass pour data. Canisters were filled typically with three glass pours from the RLFCM. The volume of the glass pour was determined from either the glass level detection system (GLDS) or the melter drop-out data. If a glass sample was not obtained, sample analyses from the preceding and subsequent pours were used to estimate the composition of all glass poured into an individual canister. Lines 46 and 48 in Appendix C present the values for cesium and strontium concentration in kilocuries, and line 49 presents the decay heat calculated from those concentrations. The method by which the total radiochemical concentration and subsequent decay heat calculations were performed is outlined in Appendix D. Also presented in Appendix D is a statistical estimation of variance in the reported values of radiochemical concentration and decay heat.

3.0 CANISTER CLOSURE

The FRG canisters were stored in B-Cell of 324 Building after being filled with borosilicate glass. Each canister was encased by an overpack with a protective lid and placed in a specially designed canister storage rack. The first steps of canister closure and decontamination were to retrieve each canister from storage, clean the lid weld surface for welding, measure the void height between the top of the glass surface and canister lid flange, calculate the void volume and place a calibrated helium capsule containing a known quantity of helium in the void space, and weld the lid onto the canister. A gross helium leak test and visual examination of the weld was then completed. The canisters were then rinsed with water to remove any loose contamination before being sent to the air lock to complete a sensitive helium leak test to verify weld integrity.

3.1 HELIUM CAPSULE FILLING

A helium leak detection system was used to verify the tightness of the lid closure weld on each canister. This was done by filling a special gas cylinder with helium which would leak at a predetermined rate. This source capsule was then placed in the void space of an FRG canister prior to welding. After welding, the capsule was allowed to build up pressure in the canister void space. The leak-tightness of the canister was then determined by checking the outside of the weld for escaping helium.

The helium source capsule (Figure 3.1) consisted of a 300-cc gas cylinder with a tapered glass capillary sealed in one end. The cylinder was filled with helium and sealed. The helium then slowly leaked out through the glass capillary. This slow leak rate ensured that the capsule would still be leaking well after the canister lid was welded. The fill pressure of each capsule was calculated using the canister void height such that once all the helium had leaked into the void space of the welded canister, the total pressure in the void would be less than 5.6 atm, the maximum allowable pressure.

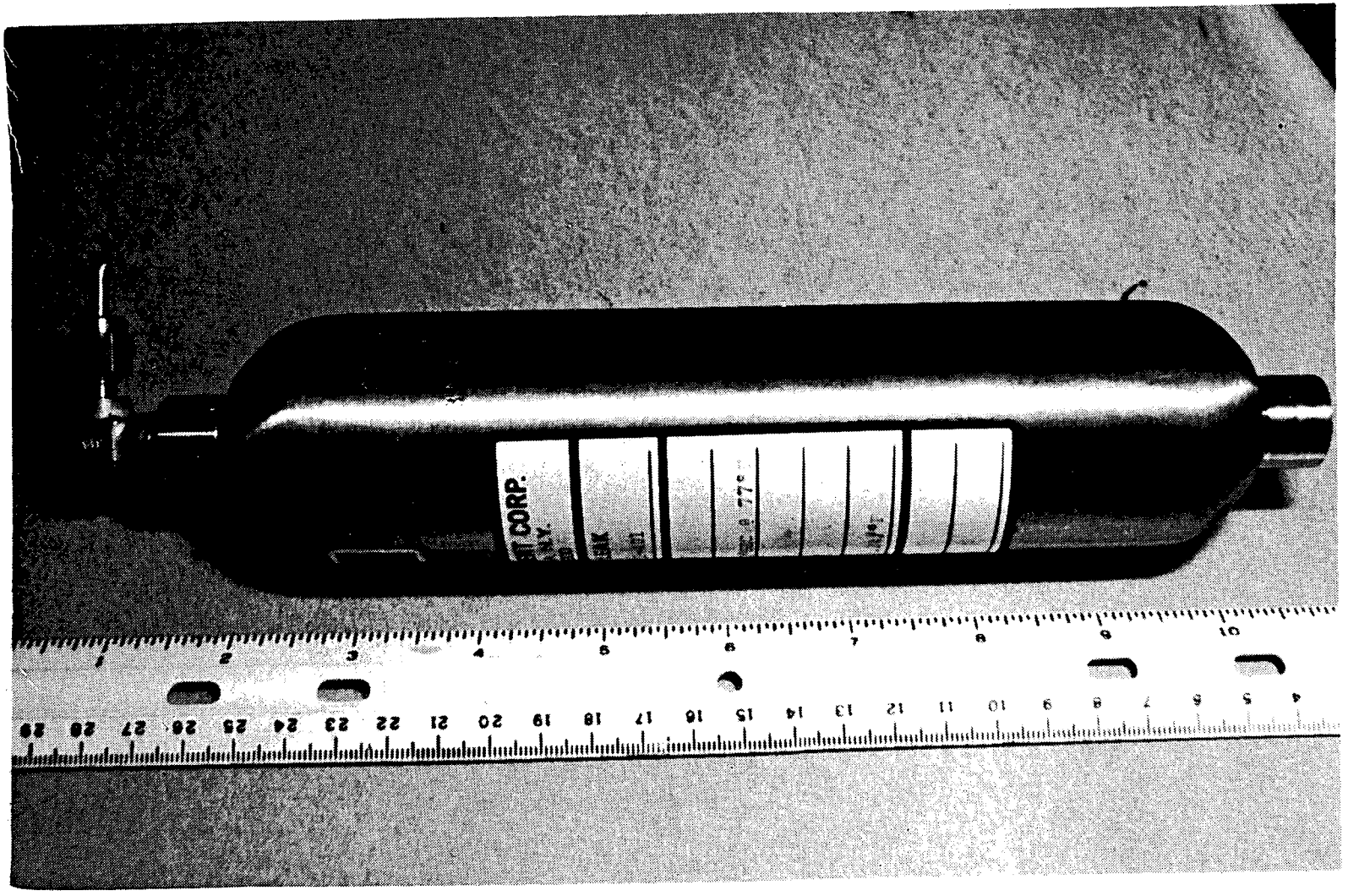

FIGURE 3.1. Helium Source Capsule

Each helium capsule was filled by mounting it to a manifold consisting of a series of valves and pressure gauges, a calibrated volume, a helium source, and a vacuum source (Figure 3.2). The capsule was calibrated by filling it with helium to 1 atm and then recording the leak rate of the helium into the calibrated volume. This was done by monitoring the pressure increase in the calibrated volume over a given time. The capsule was then filled to its final pressure (20 to 65 atm) and the leak rate was again calculated. Lines 10-12 of Appendix C contain the fill pressure, 1-atm leak rate, and fill pressure leak rate of each capsule used for the 30 canisters. Using the records of these leak rates as well as the times at which the capsule was filled, placed in the FRG canister, and welded, the canister void pressure could be calculated at any time after the canister was welded. This was done by using a computer program which will be discussed in Section 4.2.

3.2 WELD PREPARATION

Sequentially, each canister in its overpack was moved from its in-cell storage position to a weld/rinse station in B-Cell. The protective lid and the weld protector ring previously placed on the canister were then removed using a special yoke and the overhead crane.

Next the void height between the top of the glass surface and the top of the canister was measured. This was accomplished by using a ruler and measuring the depth in four places and in the center. An average value of the five measurements was determined. The void volume and its uncertainty were calculated from the void height measurement. This void volume was used in determining the fill pressure for the helium capsule (Section 3.1).

The canister flange was cleaned by using a stainless steel wire brushing wheel on a pneumatic grinder. The grinder was powered by a cylinder of breathing air located outside the hot cell. Breathing air was used to eliminate the possibility of contaminating the flange with oil or water. The inside surface of the flange near the weld joint and the top of the flange on both sides of the groove were thoroughly brushed. The groove itself was cleaned using a manipulator-held stainless steel brush. After brushing, the flange area was blown with breathing air to remove loose particulate and was visually inspected with a television camera.

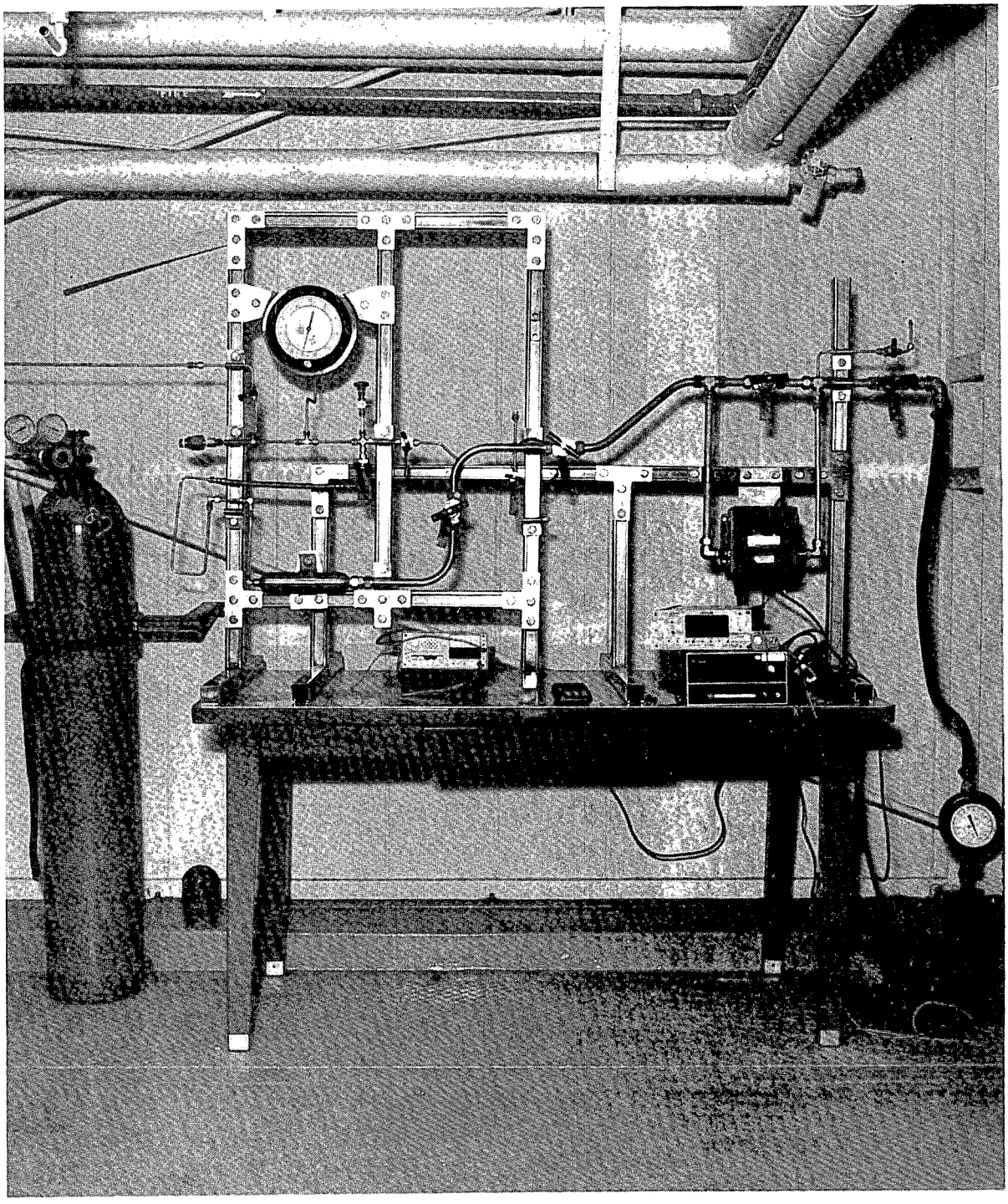

FIGURE 3.2. Helium Capsule Filling Manifold

The flange lid was thoroughly cleaned outside the cell using acetone and then alcohol. The cleaned lid and the precalibrated and filled helium capsule were then transferred into the cell. The helium capsule was placed into the canister and the lid was set on the flange. A gross helium cell background reading was taken, and then a gross helium reading was taken over the canister to assure that the capsule was releasing helium (see Section 4.1). At this point the welding head was swung over the canister lid from its storage location and lowered into position on the canister lid. Figures 3.3 and 3.4 are photographs of the welding head and welding power supply.

The weld specifications required a flange and lid temperature of 80°C to 250°C before any welding could take place. Therefore, the flange and lid temperatures were measured with a contact thermocouple. In general, ~15 min were required to heat the canister lid through contact with the canister flange to within acceptable welding temperatures.

3.3 WELDING

After the welding head had been set in place on the lid, the alignment of the electrode tip with the weld joint was checked in two locations 180° apart. This checking and any subsequent adjustment to the welding head were made by remote viewing through a Rees TV camera. Along with the electrode alignment check, the arc gap, or the distance between the end of the electrode and the canister lid, was adjusted. This was accomplished by moving the electrode down until it touched the lid. At the instant of contact, an electrical circuit was completed which turned on an audible alarm. The electrode was then adjusted upward to the predetermined arc gap distance. This distance was measured by a dial indicator mounted on the welding head which measured vertical movement of the electrode holder. After these adjustments were made and the flange and dial temperatures were determined to be within the acceptable limits, welding of the lid to the flange was begun.

Prior to lid-weld closure the lid was first tack-welded to the flange in three locations spaced 120° from each other. The final closure weld was then initiated midway between the first and last tack weld so that good visual observation could be made of the weld overlap.

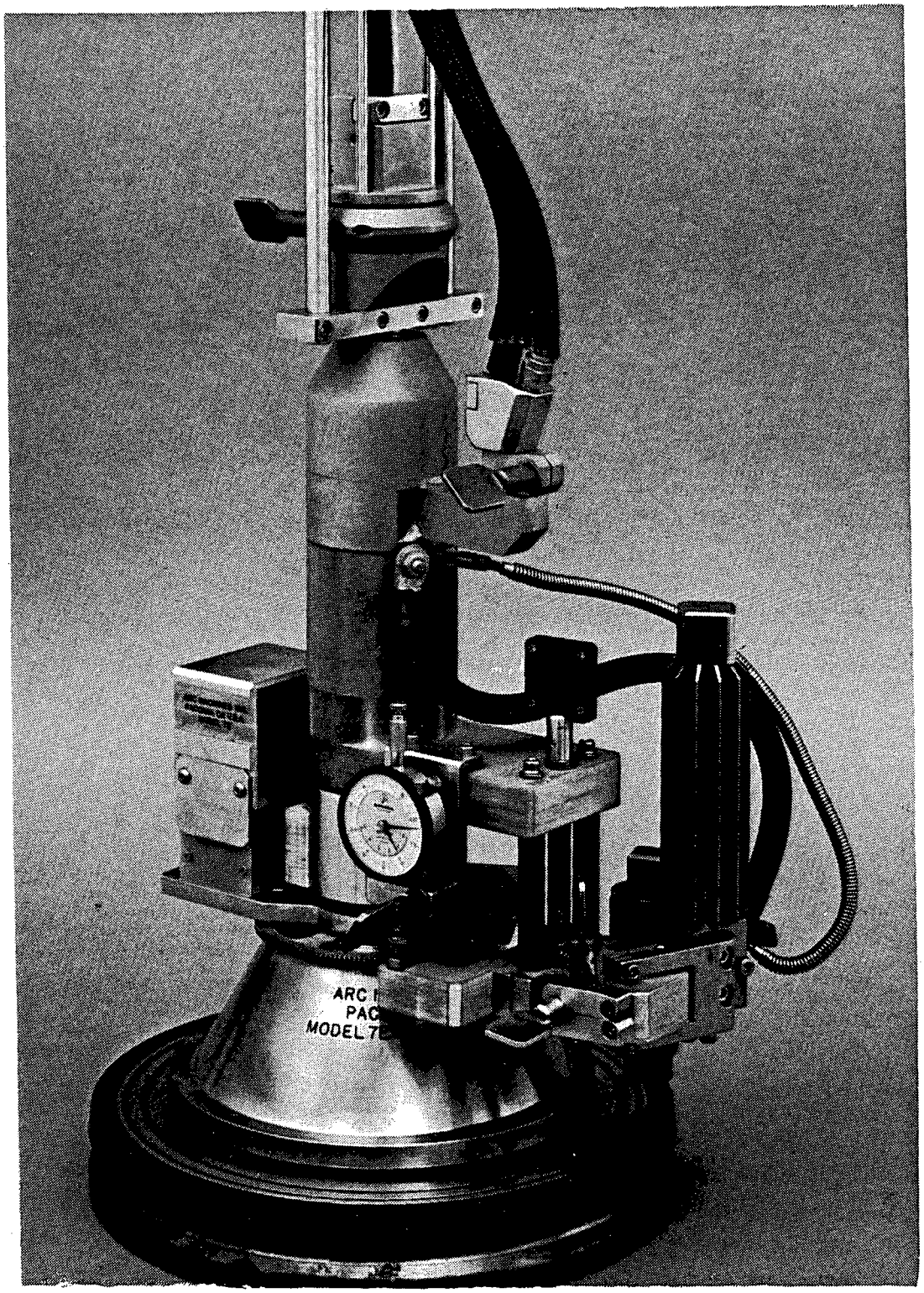

8700719-1cn

FIGURE 3.3. Remote Canister Lid Welder

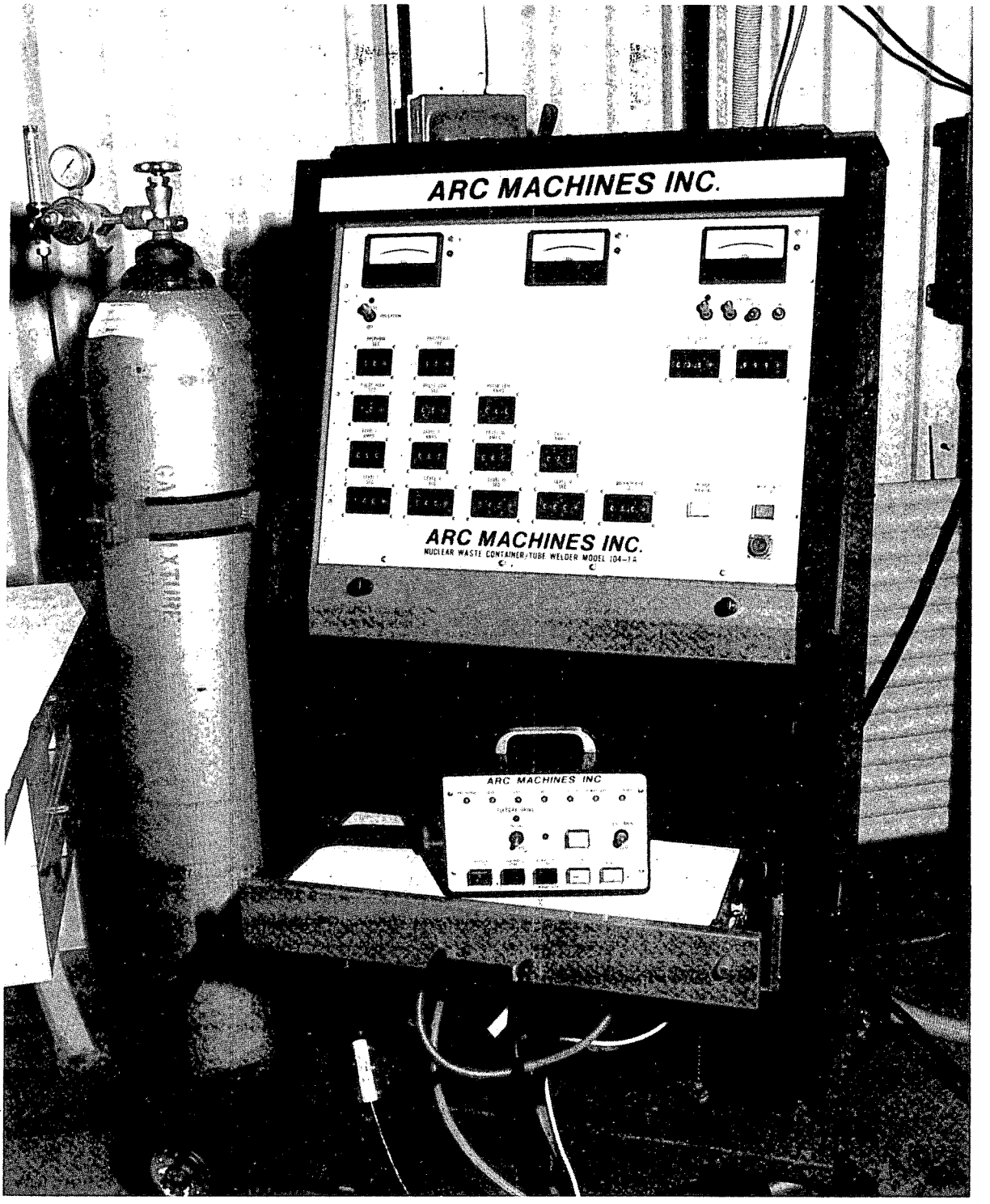

8603061-5cn

FIGURE 3.4. Welding Power Supply

The welding of the radioactive waste-filled canisters began on February 17, 1988, and was completed on March 31, 1988. Appendix C shows the date and sequence of each canister weld. The welder electrode was replaced after the seventh, fourteenth and twenty-third welds.

Welding progressed well up to the sixth canister (canister number 45), when the quality of the welding arc deteriorated. This happened after the weld had gone about halfway around the weld joint. The arc color changed to orange, and the arc expelled bits of material. After the weld was completed, the weld bead appearance was not uniform. The bead width and height varied and the bead laps were not uniform. Several test welds were made to determine the cause of the problem, but no positive determination could be made. Because experience had shown that the most likely cause was inadequate inert gas cover of the welding arc, three steps were taken to correct the problem: 1) the inert gas supply tube from the power supply to the welding head was changed, 2) the inert gas cylinder was changed, and 3) the inert gas regulator/flowmeter was changed. The welding electrode was also changed. Three test welds were made and all were acceptable.

Welding of the canisters began again and continued without incident until the fourteenth canister (canister no. 21). The welding electrode holder and electrode had been changed just prior to welding this canister. The tack welds were not normal. The arc color during the tack welds was abnormal, and weld material spattered, resulting in blackish tack welds. It was obvious that the inert gas shielding of the arc was inadequate. The inert gas supply tube between the power supply and the welding head was replaced again, but subsequent tests showed that the problem still existed. Then it was discovered that the new electrode holder was received from the manufacturer with the locating pin 180° out of position. This prevented the inert gas from entering the electrode holder. The electrode holder was replaced with one in which the pin was in the correct location. The canister tack welds were thoroughly brushed, and an acceptable canister seal weld was made. The next sixteen canisters were welded without problems. It should be noted that some weld beads contained a significant number of "slag islands," which are caused by impurities in the base metal composition.

3.4 WELD INSPECTION

During each weld, a continuous chart recording of the arc voltage, arc current, and rotational speed of the welding head was made. The date, canister number, and time of weld start was written on each recording. After each weld, the welding head was lifted off the canister lid and moved to its storage position. A gross helium leak check of the weld was then performed as described in Section 4.1. After the gross leak check was completed, a visual inspection of the weld head was performed using the Rees TV camera.

3.5 CANISTER RINSING

Each FRG canister was rinsed to remove any loose contamination before being transported from B-Cell to the Air Lock Cell. After the lid weld was inspected the canister was lifted out of the overpack using a 3.4-m-long lifting yoke attached to the B-Cell 6-ton crane. It was moved to the east end of the cell using caution to avoid contact with any material that might further contaminate the canister. The overpack yoke was attached to the 3-ton crane, and the empty overpack was moved from the welding station to its storage location. The spray cone apparatus was then placed onto the weld station and the water supply piping connected. The canister was centered over the rinse cone, and the valves to the water supply were opened. The canister was lowered and raised through the rinse cone once before being transported immediately to the air lock.

The spray cone apparatus consists of a containment vessel with a 24-in.-dia pipe ring located 2 in. down from the opening at the top. This ring is constructed of 1-in. Sch 40 pipe and contains four evenly spaced spray nozzles which are pointed inward. One other spray nozzle, located at the bottom of the rinse tank, sprays directly upward and is used to rinse the bottom of the canister.

4.0 WELD VERIFICATION

The canister lid weld was verified by performing a gross leak check in B-Cell immediately after welding. In addition, a more sensitive helium leak check was completed in a special helium leak-test vessel located in the air lock. The maximum helium leak rate specification of the canisters was 10^{-7} atm-cc/sec.

4.1 GROSS LEAK CHECK

Immediately after visual inspection of the canister lid-weld was complete, the lid weld was tested for gross leaks using a Gow-Mac™ gas sniffer (Figure 4.1). This sniffer works by drawing gas through a small hose into a thermal conductivity cell which can detect the presence of helium from leaks as small as 10^{-5} atm-cc/sec. The canister weld was tested by placing a conical section of sheet metal over the lid and then positioning the sniffer probe over a small hole located at the apex of the cone. If helium were escaping from the weld, it would rise to the top of the cone and be sampled by the sniffer. If a leak were detected, the cone would be removed and the probe would be moved slowly along the weld bead to locate the leak source. This did not need to be done as no leaks were detected on any of the 30 canisters.

Originally the entire sniffer unit was placed in B-Cell to detect gross leaks, but the high radiation exposure rates in the cell quickly damaged the system's electronics. Therefore, a new system was designed to place the sniffer unit in a shielded sample room adjacent to B-Cell (Figure 4.2). A small vacuum pump located in the sample room would draw air in from B-Cell via a small flexible hose. The sniffer probe was mounted into the pump inlet line to sample the incoming gas for helium. The exhaust from the pump was then returned to the cell to complete the closed loop. The end on the flexible hose in B-Cell was positioned over the canister in the same manner as was used when the sniffer probe was in B-Cell. This system was found to be very sensitive to helium when the flow rate of the vacuum pump was adjusted correctly. The sniffer was tested before each canister was welded

™ Tradename of Gow-Mac Instrument Co., Bridgewater, New Jersey.

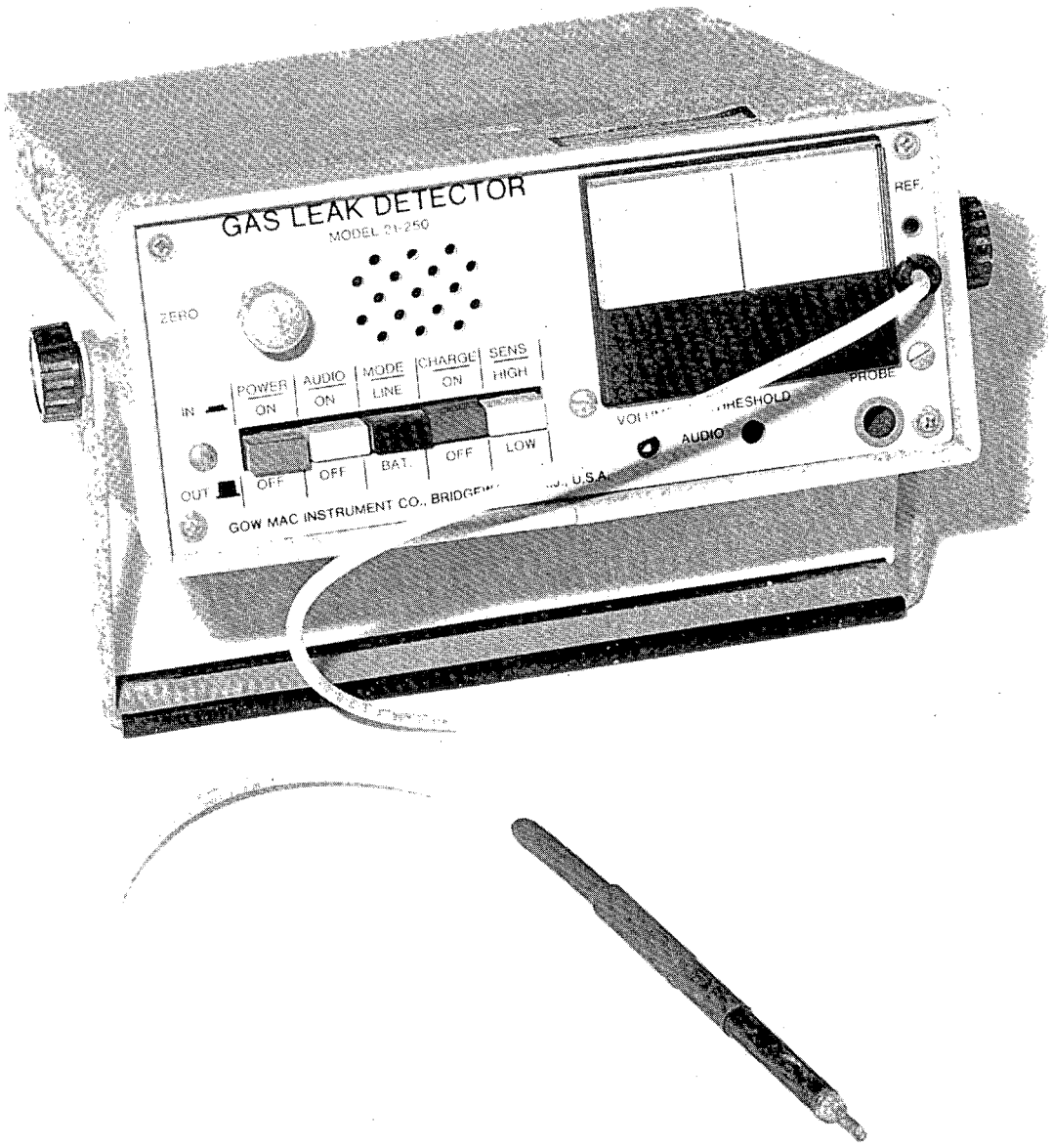

8802971

FIGURE 4.1. Gow-Mac Gas Sniffer

by placing the capsule in the canister and setting the lid in position to be welded. The conical section of sheet metal was then placed above the canister, and the sample hose was positioned above the tip of the cone. The helium escaping through the unwelded lid seam was easily detected after the capsule had built up sufficient pressure in the canister void space. The sniffer could also be tested by placing the sample hose by the GTA welder electrode and turning on the cover gas, which contained 75% helium.

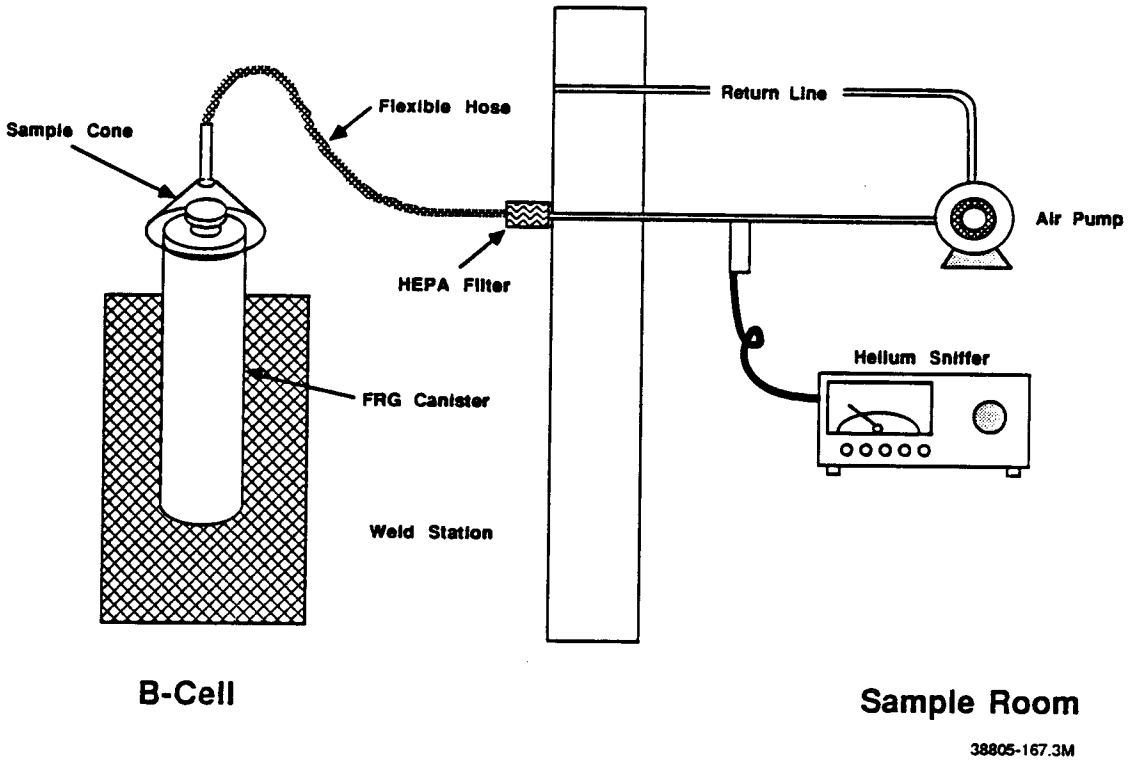

FIGURE 4.2. B-Cell Sniffer Arrangement

4.2 FINE LEAK CHECK

After the canisters were welded and rinsed in B-Cell, they were transferred to the air lock (Figure 2.1), where they remained for ~24 hr to allow sufficient helium to leak from the capsule and thereby increase the helium pressure to sufficient levels in the canister void space. The canisters were then subjected to a more sensitive leak test in which they were sealed inside a 160 L cylindrical vacuum vessel (Figure 4.3). The vacuum vessel was then evacuated and the effluent tested for the presence of helium using a mass spectrometer leak detector that detects leak rates as low as 10^{-9} atm-cc/sec.

Before each canister was tested, the leak detector was calibrated using a standard helium source capsule with a known leak rate to determine the sensitivity of the detector. This leak was connected to the detector, which was outside the air lock. The sensitivity of the detector was normally ~5 x 10^{-10} atm-cc/sec/unit (Line 17 of Appendix C). The entire system was calibrated once each week by placing another standard leak inside the vacuum vessel in the air lock and evacuating the vessel. The response of the leak

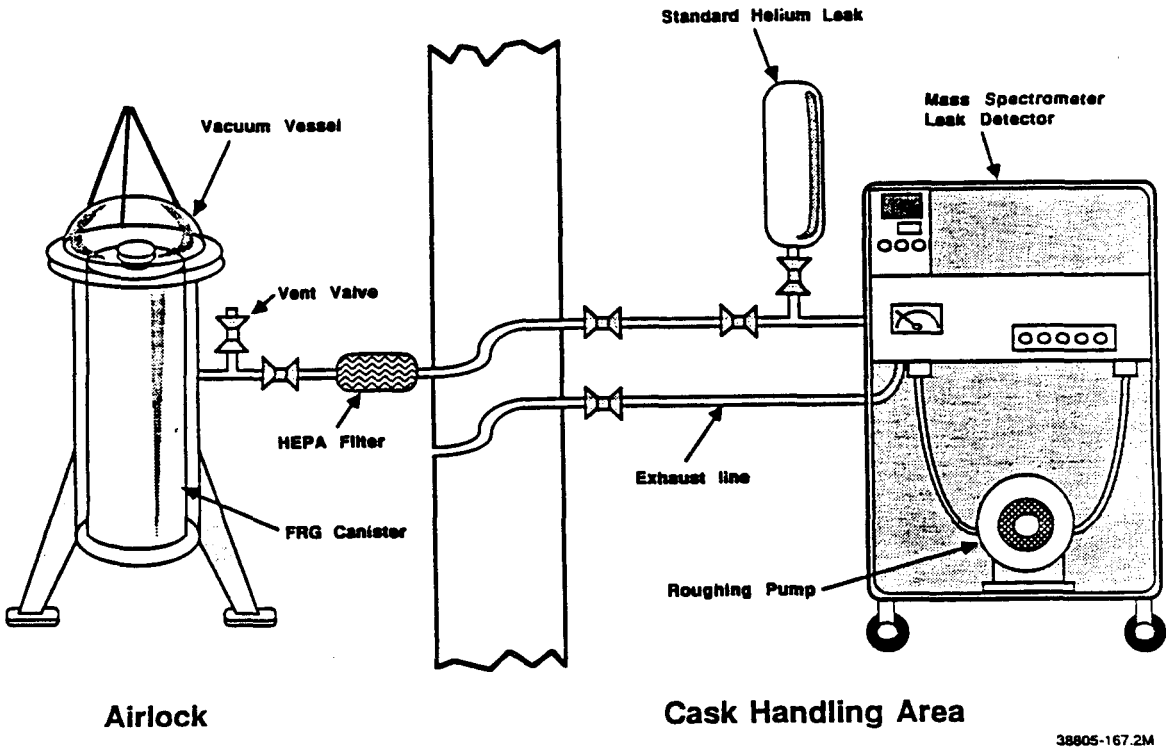

FIGURE 4.3. Helium Leak Detection System

detector was used to calculate the experimental leak rate of the source, and this was compared to the actual value. The actual standard leak rate was 5.7×10^{-8} atm-cc/sec, and the value calculated each week was between 5 and 7×10^{-8} atm-cc/sec.

Each FRG canister was tested by placing it in the vacuum vessel and sealing the vessel lid. The vessel was then evacuated down to 10 μm of mercury using the roughing pump on the leak detector. This step usually took 1 to 2 hr because of the size of the vessel and the length of tubing connecting the vessel to the detector. When the pressure was below 10 μm, the effluent stream was shifted to the mass spectrometer and the pressure was reduced below 1 μm using a diffusion pump. A gross leak rate could then be calculated by comparing the response of the detector for the canister to that of the detector to the standard leak. The canister was then removed from the vacuum vessel, and the lid of the vessel was resealed. The empty vacuum vessel was then evacuated and shifted to the mass spectrometer in the same manner as when the canister was in it. The response of the leak detector to the empty vessel was recorded and converted to a leak rate. This served as a

background for the system. The net leak rate for the canister was then calculated by subtracting the background for the empty vessel from the gross leak rate. The net leak rate is the portion of the gross leak rate attributed to the canister.

The vacuum vessel backgrounds, gross leak rates, and net leak rates for the 30 canisters are tabulated in lines 18, 19, and 20 of Appendix C, respectively. The average net leak rate for the 30 canisters was 2.4×10^{-9} atm-cc/sec, and the maximum value was 2.4×10^{-8} atm-cc/sec. This value is well below the maximum allowable FRG limit of 10^{-7} atm-cc/sec. It should be noted that the net leak rate is negative for 5 of the 30 canisters. This occurred because the vacuum vessel had to be vented between the background and gross leak rate readings so that the canister could be removed from it. For these five canisters it apparently caused a change in the vessel background reading, but the differences were very small.

A computer program was written to calculate the canister void pressure versus time when given the canister void volume, helium capsule characteristics, capsule filling time, capsule emplacement time, and welding time. This program was used to determine the time required before the helium capsule had built up enough pressure in the canister void to allow leak testing. The program also converted the experimentally determined leak rate to the leak rate that would be observed if the canister were at ambient conditions of 25°C and 1 atm differential pressure. This was done because the specified criterion of 10^{-7} atm-cc/sec maximum leak rate was at ambient conditions and not at the conditions of the individual canisters. The computed canister void pressure, capsule pressure, and converted leak rate at the time of leak detection are shown in lines 30, 31, and 32 of Appendix C, respectively.

A second computer program was written to determine the equivalent measurable leak rate which would be present at the time of leak detection for the given conditions of each canister (void temperature and pressure and capsule pressure) if an actual leak with a leak rate of 10^{-7} atm-cc/sec at ambient conditions (25°C and 1 atm) were present. These calculations were then repeated for a leak rate of 10^{-8} atm-cc/sec at ambient conditions. The results of these computations are shown in Figure 4.4. This graph shows

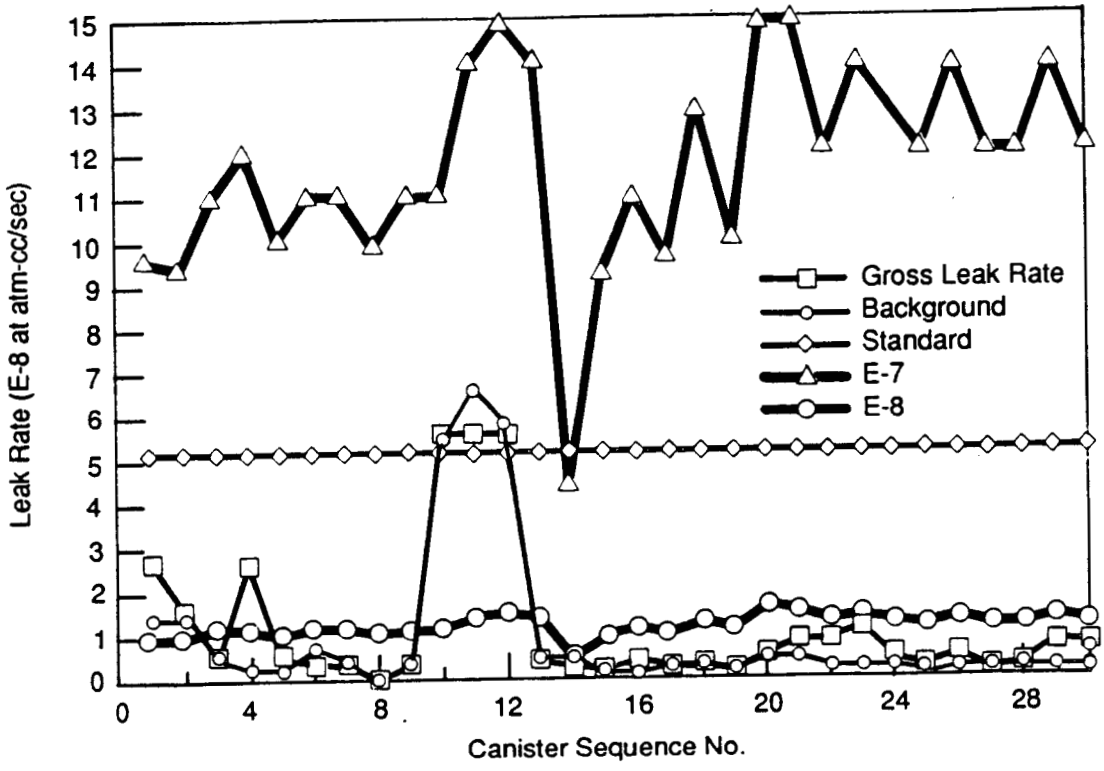

FIGURE 4.4. Leak Detection Computation Results

canister sequence number versus the various leak rates. The canister sequence number is not the actual canister serial number, but the number assigned to each canister in terms of when it was processed. The leak rates are at the conditions (temperature, void pressure, viscosity, etc.) of the various canisters and not at ambient conditions. The line labeled E-7 represents the equivalent measurable canister leak rate for a 10^{-7} atm-cc/sec leak at ambient conditions, and the line labeled E-8 represents that for a 10^{-8} atm-cc/sec leak at ambient conditions. For instance, if a canister had a 10^{-7} atm-cc/sec leak rate at 25°C and 1 atm differential pressure, what would this leak rate be at the actual testing conditions of 300°C and 0.8 atm differential pressure of canister 19? Again, this was done because the specified criterion of 10^{-7} atm-cc/sec maximum leak rate was at ambient conditions and not at the conditions of the individual canisters. Plotted against this group of data are the gross leak rate, the vacuum vessel background, and the standard leak reading. The standard leak reading shown on the graph is the standard helium leak used to calibrate the leak detector each day. This standard has a constant leak rate of 5.2×10^{-8} atm-cc/sec,

which generally corresponded to a leak detector reading of 100 units. Therefore, the sensitivity of the leak detector was in the range of 5×10^{-10} atm-cc/sec/unit.

Two anomalies are shown in Figure 4.4. The first is the unusually high gross leak rates and background leak rates for canisters 10 through 12. This was due to some contamination in the vacuum vessel which caused a high background reading. It did not pose a problem because the net leak rate (gross minus background) was still near zero. The second anomaly is the low equivalent measurable leak rate calculated for the 10^{-7} atm-cc/sec leak rate of canister 14. This was due to a low void pressure in the canister at the time of leak detection. This low equivalent measurable leak rate was far above the leak detector's limits and would have been easily detected.

Figure 4.4 confirms that all canister leak rates were well below the requirement of 10^{-7} atm-cc/sec, and in most cases one to two orders of magnitude lower. The graph shows also the leak detector was so sensitive that any actual leak rate above 10^{-8} atm-cc/sec at ambient conditions would have clearly been seen for the given conditions of each canister when tested.

5.0 ELECTROPOLISHING

Electropolishing technology was used to decontaminate the top, sides, and bottom of the FRG canisters. The specifications for smearable contamination on the FRG canisters required the surface contamination to be below 22,000 dpm/100 cm^2 (370 Bq/100 cm^2) beta-gamma and 2200 dpm/100 cm^2 (37 Bq/100 cm^2) alpha.

5.1 ELECTROPOLISHING SYSTEM DESCRIPTION

The 30 filled and sealed FRG canisters were decontaminated using an electropolishing system located in A-Cell of the 324 Building (Figure 2.1). Shown in Figure 5.1 is the associated equipment arranged in the decontamination cell. This equipment included the electropolisher, an equipment storage rack, and a water-cooled storage vessel in which the canisters were placed after electropolishing. The major components of the electropolishing system are shown in Figure 5.2. The electropolishing tank constructed from Hastelloy C-276® could hold up to 1000 gal of electrolyte and was provided with systems for heating, cooling, filtering and mixing of the electrolyte. The electrolyte used was 85 wt% phosphoric acid.

The following paragraphs briefly explain the electropolishing process as it was performed in A-Cell. The first A-Cell operation was to retrieve the canister from the A-Cell door transfer cradle and place the canister in the electropolisher.

The first electropolishing step was to electropolish the canister lid at a power setting of 1000 amperes for 10 min. The electrical contact to the canister was through the lower electrode, on which the canister sits. The canister lid was located in the center of the cathode ring when the canister was in this position.

The next step was to electropolish the bottom of the canister. This was accomplished by first connecting the anode grapple to the canister, which was then sitting on the lower electrode of the cathode cage. The canister was then raised 15 cm above the lower electrode, and the bottom was

® Registered trademark of Cabot Corporation, Kokomo, Indiana.

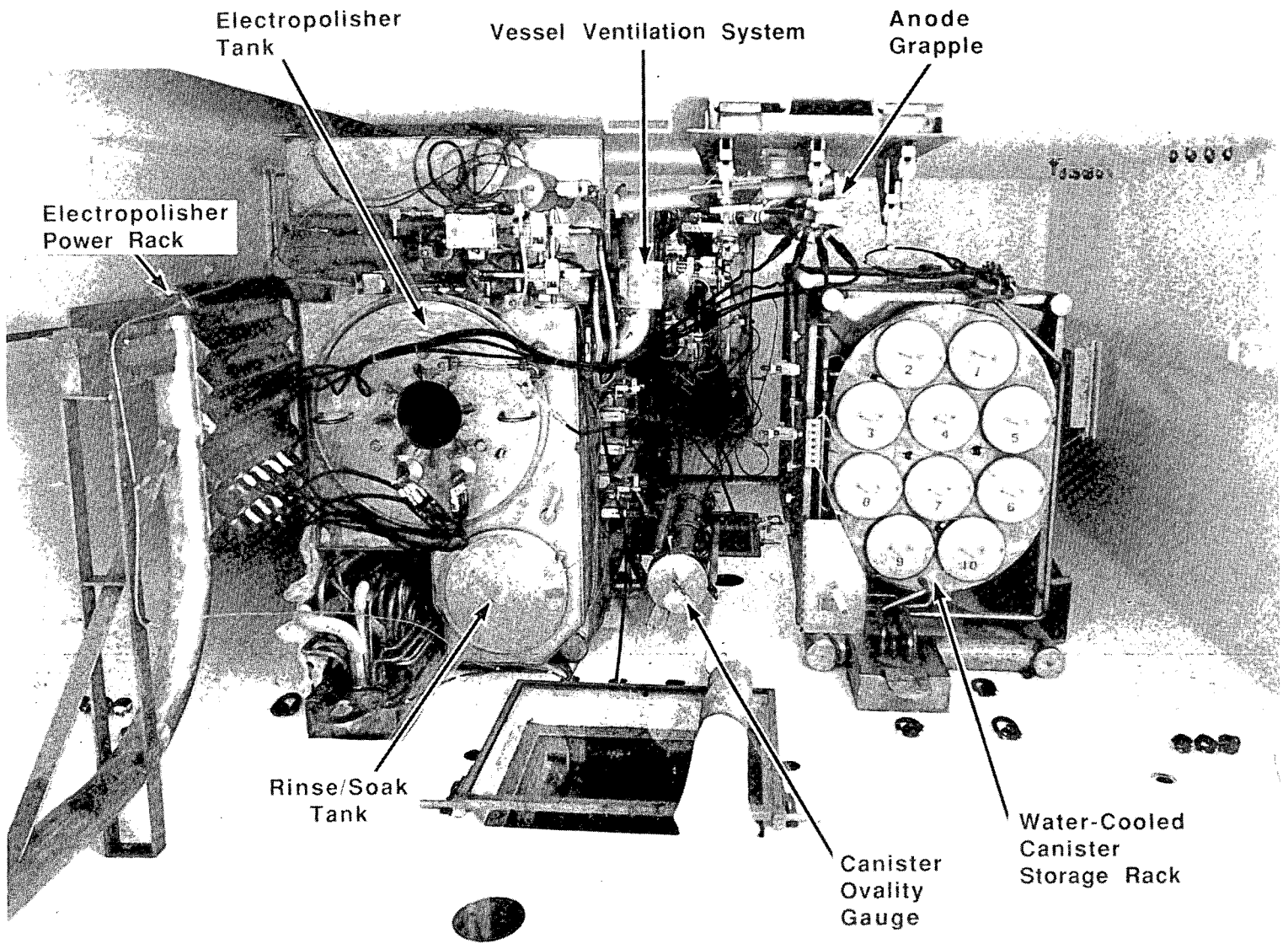

8800318-6cn

FIGURE 5.1. Overhead View of the Canister Decontamination Cell

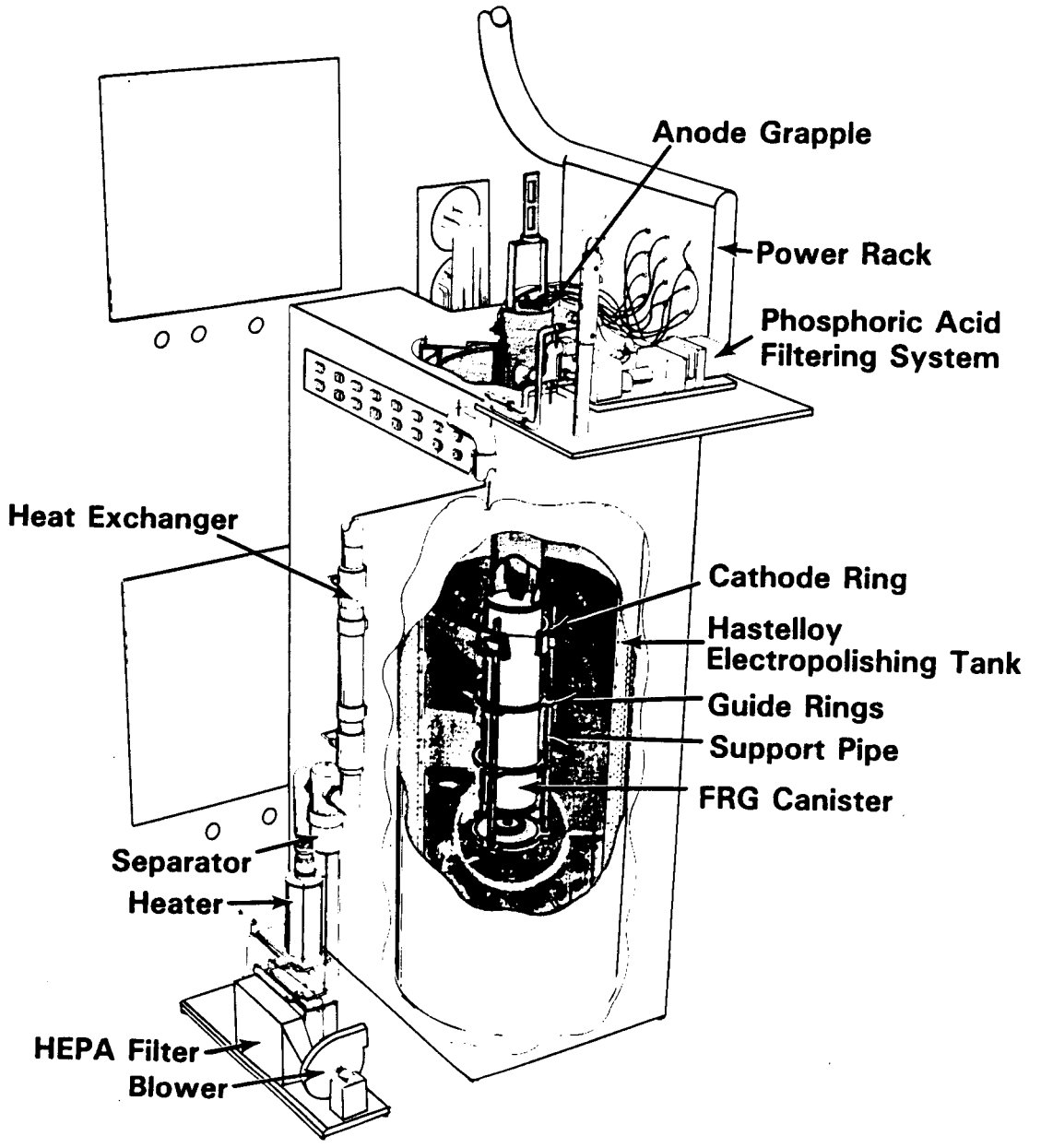

FIGURE 5.2. Canister Electropolishing System

electropolished for 10 min at 1000 amperes set on the power supply. The level of the canister was determined by reading the calibration on the side of the anode grapple which directly corresponds to the spacing between the bottom of the canister and the lower electrode.

The last step in this process was to electropolish the canister walls in two stages. The first stage involved electropolishing the canister at high

current densities and the second at a low current density. The power supply was operated at 500 amperes for the first stage of operations and at 100 amperes for the second. In the first stage, the actual decontamination is accomplished by removing ~1 mil (0.25 μm) of the canister's surface metal. The second electropolishing stage was an etching mode, during which the canister surface is dulled to enhance the emissivity of the canister surface. Emissivity is a heat transfer property important in the exchange of radiant thermal energy from one surface to another. The specifications for the FRG canisters call for an emissivity of greater than 0.4 to provide for adequate heat transfer in the canister shipping cask. With the etching of the surface this specification can be achieved. The canister wall is electropolished by sequentially raising and lowering the canister through the cathode ring. The anode grapple completes the anodic circuit to the canister, and the counter electrode is the ring in the cathode cage. The cathode ring is 15 cm in height; therefore, the canister must be raised or lowered in 15-cm increments to electropolish the canister wall.

The electropolishing of the canister wall in the first of the two stages is completed in two passes. In the first pass the canister is sequentially raised through the cathode ring in 15-cm increments. At each incremental position the electropolisher is operated for 5 min at a power supply setting of 500 amperes. In the second pass, at the same power setting and time, the canister is lowered back through the cathode ring. However, the canister is first lowered 7.5 cm so that each incremental position is offset by 7.5 cm as the canister is passed back through the cathode ring, resulting in a more uniform finish on the final electropolished surface.

The etching of the canister surface is the final electropolishing step. To etch the canister walls, the canister is lowered incrementally through the cathode ring as was done in the second pass of stage one above. The power supply setting is 100 amperes, and etching time is 15 min at each incremental position. Only one pass through the cathode is required for this step.

One final step in the process is required before the canister is removed from the electropolishing tank (EPT). This is to electropolish the lid for 1 min at 500 amperes to remove any acid residue which may have adhered to it.

The canister is then raised from the cathode cage through an air/water spray originating from the spray ring in the upper portion of the EPT. To provide adequate time for rinsing the canister wall, the crane is operated at low speed while raising it through the spray ring. The canister is then transported to the rinse/soak tank (RST) and lowered to the bottom. The bottom of the canister is then rinsed using the spray nozzle on the floor of the RST. The final rinse of the canister is then completed using the spray ring of the RST. This is done by slowly raising the canister through the RST spray ring as was done when rinsing the canister in the EPT.

After rinsing in the RST, the canister was allowed to dry and a smear test of the canister was completed. The smear test was conducted using a special smear pad holder, held with a manipulator, and moved a fixed distance along the canister side. The smear pad was held by double-sided tape in a preformed holder. Fiberfrax felt was used as the smear pad because of its resistance to the high temperature of the canister side wall. The smear pad (diameter 5 cm) was moved 30.5 cm along the axis of the canister, as monitored by a gauge. The total smeared area was 175 cm^2.

Gamma activity on the smear pads from ^{137}Cs decay products was counted with a GeLi detector in a shielded cave. The beta activity from ^{90}Sr was counted using a mini-scaler and external detector apparatus borrowed from laboratory radiation protection services. The beta activity was counted on 5-cm-dia air sample filters. The sample holder positions of the smear pad are very close to the detector so as to capture the short-range beta particles. Alpha activity was determined with a ZnS scintillation detector designed for counting samples shaped like the smear pads.

5.2 ELECTROPOLISHING RESULTS

The electropolishing system operated very well for the period during which the 30 FRG canisters were decontaminated. The canisters received in A-Cell were highly oxidized with high levels of smearable contamination on the surface. Figure 5.3 shows a typical canister before electropolishing and Figure 5.4 shows an electropolished canister. The electropolishing process removed all the oxide coating the canister surface and decreased the levels

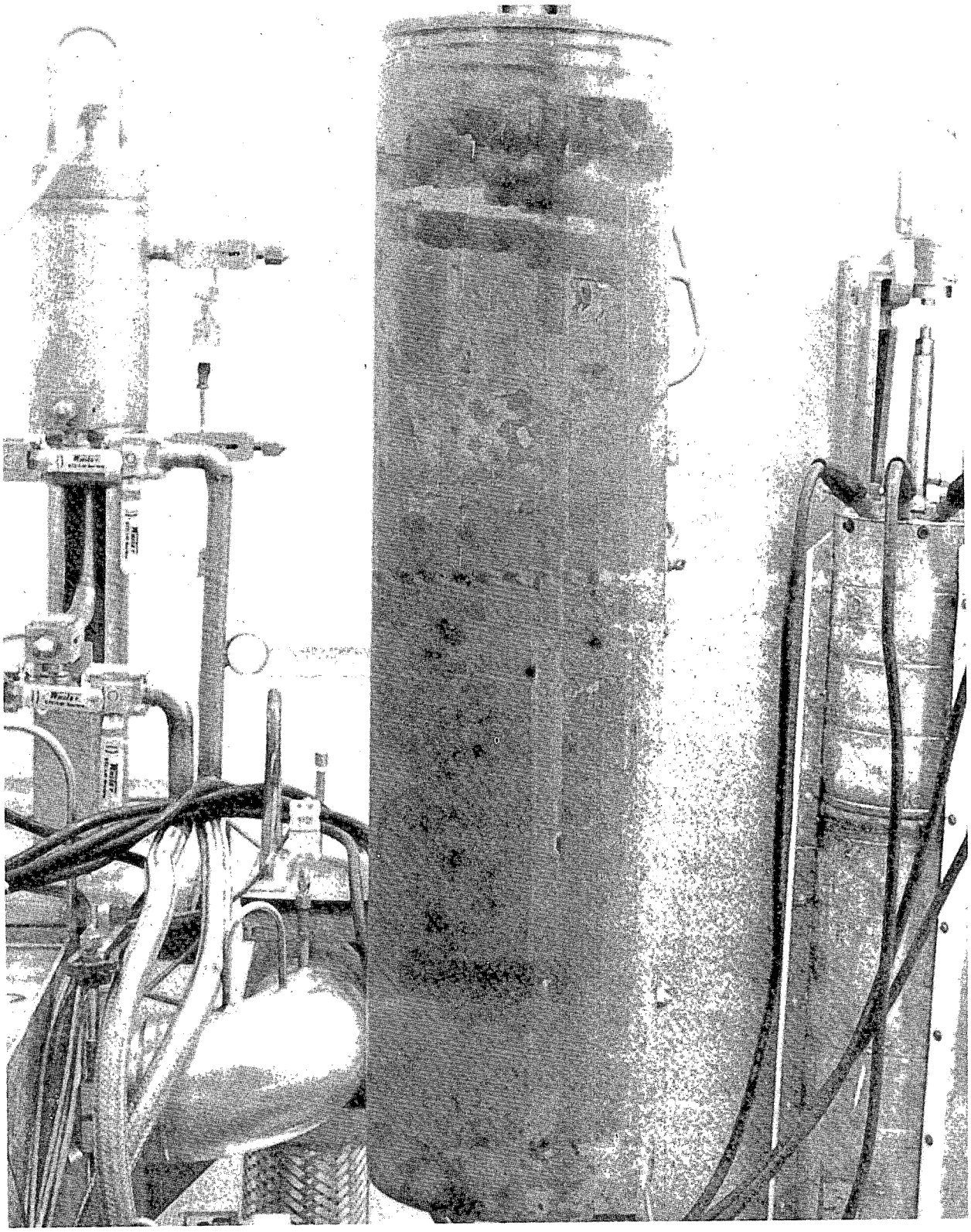

8801760-2cn

FIGURE 5.3. Radioactive Canister Before Electropolishing

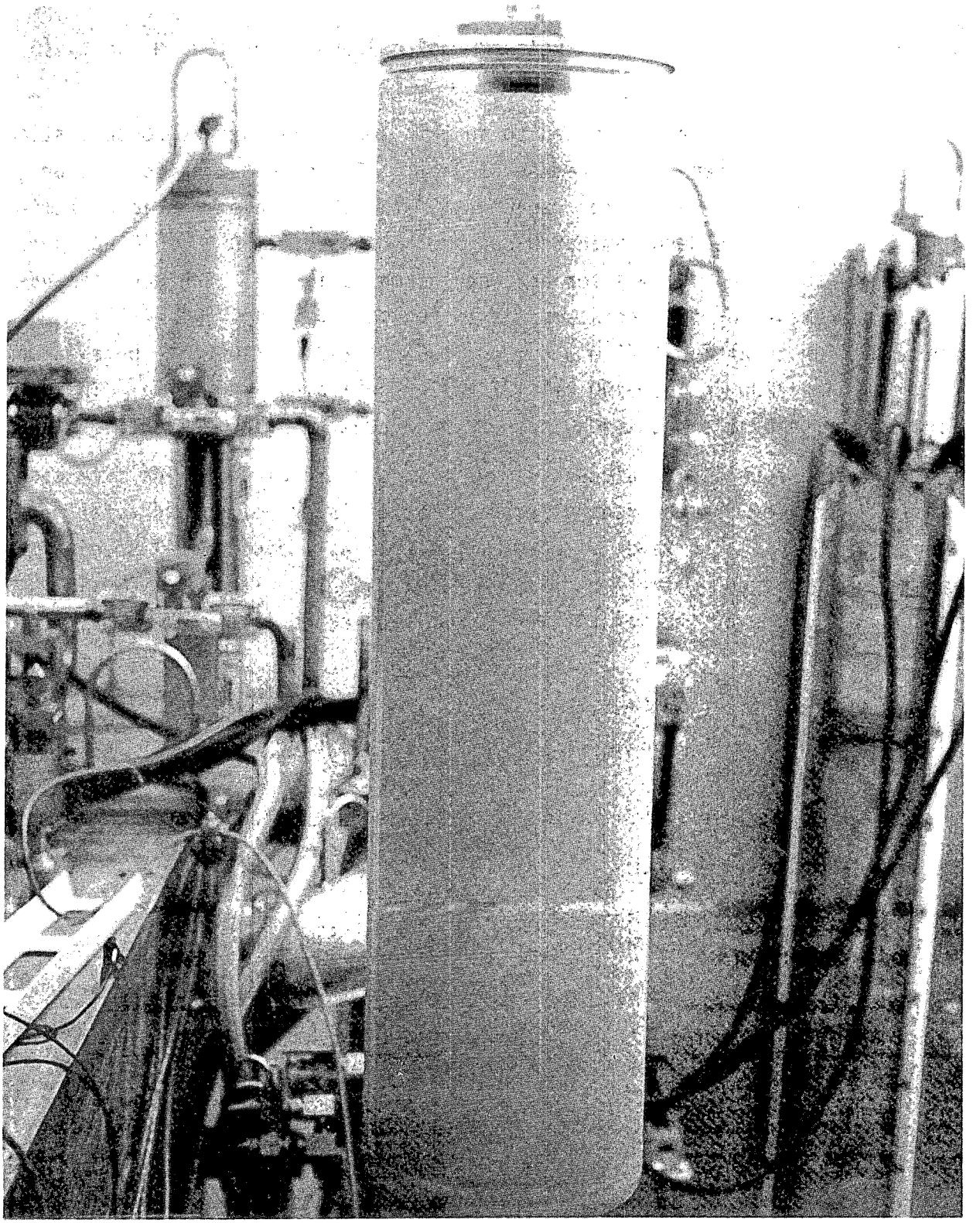

8801760-1cn

FIGURE 5.4. Radioactive Canister After Electropolishing

of smearable contamination to levels averaging 300 dpm per 100 cm^2 units (5 Bq/100 cm^2).

The canisters were determined to contain smearable surface contamination in the range of 1 mrem to 60 mrem per 100 cm^2. The decontamination factor (DF) for the process was in the range of 10^3 to 10^5. The smearable contamination levels on the decontaminated canisters ranged from 0 to 2000 dpm per 100 cm^2 (0 to 33 Bq/100 cm^2) for beta and gamma radiation. The decontamination requirement for the canisters was to reduce the smearable surface contamination to at least 22,000 dpm per 100 cm^2 (370 Bq/100 cm^2) beta-gamma radiation and 2200 dpm per 100 cm^2 (37 Bq/100 cm^2) alpha radiation. The actual results of the process surpassed this requirement by a factor of 100.

The electropolishing process removed ~1 kg of metal and oxide from each canister surface, as measured by weighing the canister before and after electropolishing. The level of chemical as well as radiochemical species was monitored throughout operation of the electropolisher. Table 5.1 presents the concentration of the various constituents detected in the electrolyte solution.

The total metals concentration in the acid after the 30 canisters were electropolished was 0.8 wt%. Previous electropolishing experience has shown

TABLE 5.1. Concentration of Constituents in Electrolyte Solution

Sample #	Number of Canisters Processed	Fe, ppm	Ni, ppm	Cr, ppm	^{137}Cs, Ci/Liter
1	1	647	1280	365	--
2	5	703	1685	455	--
3	9	945	3057	790	1.86×10^{-6}
4	18	2138	2908	1062	5.95×10^{-6}
5	22	3475	3137	1405	1.05×10^{-5}
6	25	4173	3603	1695	1.20×10^{-5}
7	27	4502	4328	1933	1.29×10^{-5}
8	30	4373	4503	1932	1.35×10^{-5}
9	32	5700	4543	2229	2.10×10^{-5}
10	33	6627	3568	2221	5.72×10^{-5}

that an electrolyte is useful up to metal concentrations of 10 wt% metals. From the experience gained in the electropolishing of the FRG canisters it was shown that a total of 375 canisters could be decontaminated based on the accumulation of metal in the acid.

The accumulation of radiochemical species in the electrolyte was monitored as indicated in Table 5.1. After electropolishing 30 canisters, there was a total of 3×10^{-2} Ci ^{137}Cs in the 2200 L of phosphoric acid. This value translates to a contamination level on each canister of 1×10^{-3} Ci ^{137}Cs/canister.

After electropolishing, the general appearance of the canister surface could be characterized as an even "matte" or dull finish. The finish did, however, vary from canister to canister. It was not determined why some canister surfaces were not dulled to the same degree as others. Generally, however, the seven canisters that were preelectropolished appeared less dull than the others. The appearance of all 30 canisters was very similar to that of the one on which emissivity measurements were obtained. It was measured at greater than 0.4.

The top and bottom of the canisters appeared to have all oxides removed. A smear of the canister bottom was obtained to assess the smearable contamination level after electropolishing. This surface smeared well below the specifications for the FRG canisters.

All 30 FRG canisters were placed in a water-cooled storage vessel on completion of electropolishing operations. The water-cooled storage rack (WCSR) consists of an elliptical vessel with an array of 10 vertical tubes in which the canisters are stacked three high. Water is circulated past the array of tubes to dissipate the decay heat of the canisters. After all 30 canisters were placed in the storage rack, the cooling water flow rate was adjusted to 20 L per minute. At this flow rate the inlet and outlet temperatures were 15 and 42°C, respectively. The cooling water removes ~38 kW of decay heat from the WCSR. The total decay heat generated from the 30 canisters is ~47 kW. This indicates that 20% of the decay heat is lost to the cell air through convection from the tank surface.

6.0 CANISTER CHARACTERIZATION

Each FRG canister was nondestructively characterized by measuring the surface radiation exposure rate, surface temperature, canister weight, ovality and straightness by passage through a go-no go gauge, gamma spectrum, and smearable surface contamination level. The surface temperature and exposure rate were measured before the canisters were electropolished, and the canister weight, ovality, gamma spectrum, and smear test were completed after electropolishing.

6.1 EXPOSURE RATE MEASUREMENTS

The decay of ^{137}Cs in the glass generates a gamma flux at the surface of the canisters. This flux was measured in terms of Roentgens per unit time (R/hr). The following sections describe the equipment used and the methods for handling data to determine exposure rates.

6.1.1 Equipment Description

The equipment for measuring the canister exposure rate consists of ion chamber probes, power supplies, electrometers for measuring passage of current, thermocouples for the probes, and a holder for the probes in the remote cell. Figure 6.1 gives a schematic of the system.

Three probes were used: two are designed for use in a reactor core and are manufactured by Reuter-Stokes, and the other is for medical radiology applications and is manufactured by Exradin. The Reuter-Stokes chambers are 6.4 mm dia by 76 mm long, with a 0.033-mm-thick steel chamber wall. The Exradin chamber is spherical with a volume of 3.6 cc and is constructed of plastic. The ion chambers are filled with gas which becomes ionized when subjected to gamma photons. Ionized species migrate to electrodes in the chamber which are polarized by the power supply. The collected ions register as current on a microammeter (or electrometer). This current is converted to exposure rate using calibration data.

The Reuter-Stokes probes were alternately connected to the same direct current power supply and electrometer during measurements. The Exradin probe had an independent power supply (a 300 V dry-cell battery) and electrometer.

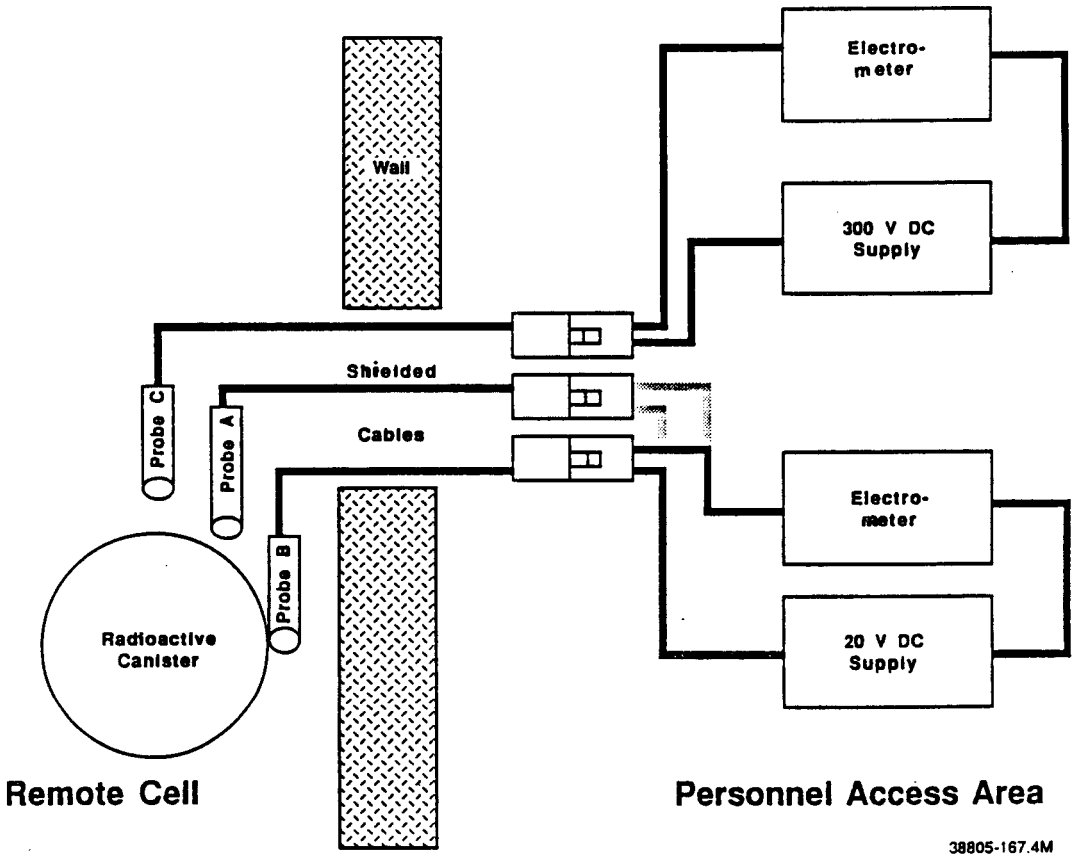

FIGURE 6.1. Schematic of Exposure Rate Measurement System

Probe chambers were positioned at fixed distances from the FRG canisters using an adjustable holder attached to the helium detection vessel. Also, one of the core chambers was held against canisters with a manipulator. Reuter-Stokes chamber temperatures were measured with a thermocouple and displayed on a digital thermometer. During measurements, each probe was connected in series with a power supply and electrometer.

6.1.2 Conversion of Probe Current to Exposure Rate

Current induced in the ion chamber probe by radiation from FRG canisters can be converted to an exposure rate using calibration data. The following empirical relation is used:

$$D = (y - y' - \sigma) / \alpha \qquad (1)$$

where D is measured exposure rate, y is measured current in amperes, y' is leakage current, and α and σ are coefficients. Values of α, σ, and y' for all probes are shown in Table 6.1. The two Reuter-Stokes probes were operated at 20 V dc and are designated A and B. The Exradin probe was operated at 300 V dc and is designated C. Leakage current is the current through the probe/power supply/electrometer circuit in the absence of gamma flux and was measured after the probes were installed in the remote cell.

Values of α and σ for probes A and B were based primarily on vendor-supplied calibrations at 8,700 R/hr, 100,000 R/hr, and 2,100,000 R/hr. The slightly nonlinear exposure-current response was linearized using different sets of α and σ for the low range (8,700 R/hr to 100,000 R/hr) and the high range (100,000 R/hr to 2,100,000 R/hr). Once all measurements were made, it was found that probe A readings were consistently higher than probe B readings and that the average relative error for all exposure rates was about 10%. The consistent variation between probes A and B suggested that the vendor-supplied conversion parameters were inaccurate. Values for α and σ were then varied by successive trials until a minimum average relative error was found. These adjusted values are shown in parentheses in Table 6.1. The average relative error was reduced from about 10% to 5% using the adjusted conversion parameters.

During measurements, probes A and B were usually heated by FRG canisters to about 40°C but never exceeded 65°C. Room-temperature calibration data were used, however, because α and σ are insensitive to temperatures below 100°C.

For probe C, calibration was done at PNL with one exposure rate of 66,000 R/hr and at room temperature only. The parameter σ is indeterminate and is presumed to be zero. The value for y' was found to be less than 10^{-13} amp, and was also considered to be zero in the calculations. No adjustment of α and σ for probe C was needed.

During measurements, current from probes A and B generally ranged from 0.2×10^{-9} amp to 1.5×10^{-9} amp. For probe C, the current was higher because of greater sensitivity and was in the range of 0.8×10^{-9} amp to 10×10^{-9}.

TABLE 6.1. Parameters To Convert Current to Exposure Rate at Room Temperature[a]

	8,700 to 100,000 R/hr	100,000 to 2,000,000 R/hr
Probe A, 20 Volts		
α, amp/R/hr	5.05×10^{-15} (5.30×10^{-15})	4.72×10^{-15} (5.30×10^{-15})
σ, amp	8.36×10^{-12}	3.84×10^{-11} (4.84×10^{-11})
y', amp	9.00×10^{-11}	9.00×10^{-11}
Probe B, 20 Volts		
α, amp/R/hr	5.60×10^{-15} (5.00×10^{-15})	5.19×10^{-15} (5.00×10^{-15})
σ, amp	8.39×10^{-12}	4.23×10^{-11} (2.20×10^{-11})
y', amp	9.00×10^{-11}	9.00×10^{-11}
Probe C, 300 Volts		
α, amp/R/hr	4.08×10^{-14}	4.08×10^{-14}
σ, amp	0	0
y', amp	0	0

(a) Values not in parentheses were obtained by initial calibration using known gamma sources. Values in parentheses have been adjusted to minimize the relative standard error between all measurements. The adjusted values were used to report canister exposure rates, rather than the corresponding initial calibration values.

6.1.3 Distance Correction

Probes were located some finite distance X from the canister surface. It is necessary to correct measurements made at a distance to a surface exposure rate. Based on analysis of the results from the computer code

ISOSHLD, the following relation is found to describe the dependence of exposure rate versus distance from FRG canisters for distances less than about 15 cm:

$$D = \frac{D_o}{1 + hX} \tag{2}$$

where D_o is surface exposure (R/hr), h is a coefficient with a value of 0.095 cm^{-1} and X is distance between the center line of the probe and the surface of the canister. The radius of all three probes is about 3.2 mm. The value for X is given by the distance between the outside of the probe and the canister plus the radius of 3.2 mm. The distance from the probe wall to the canister varied from 0 cm (probe held against canister) to 16.2 cm. Most measurements were done with one probe against the canister (probe B), one at 1.5 cm from the canister (probe A), and one at 2.5 cm from the canister (probe C). To determine D_o, Equation (2) is rearranged:

$$D_o = (1 + hX)D. \tag{3}$$

6.1.4 Exposure Rate Results

The results from measuring the 30 canisters containing ^{137}Cs and ^{90}Sr isotopes are given in Table 6.2. The reported exposure rate is generally an average of three probe measurements that have been extrapolated to a surface exposure using Equation (3). The range of exposure rates is 26,000 R/hr (canister 44) to 320,000 R/hr (canister 48). The standard deviation is calculated using the variance and t-values from the "Students" distribution. All but eight canisters have surface exposure rates in the range of 218,000 R/hr to 320,000 R/hr.

6.2 TEMPERATURE SCAN

The axial surface temperature profile of each canister was taken while the canister was in the air lock prior to leak checking. The temperature was taken at five equidistant points along each canister using the canister surface temperature probe (Figure 6.2) and the temperature probe alignment

TABLE 6.2. Measured Radiation Exposure Rates at Surface of FRG Canisters

Canister Number	Mean Surface Exposure, R/hr x 10^3	Standard Deviation, 95% Confidence Limit, R/hr
1	236	22.7
2	266	--
3	233	15.6
5	273	8.8
6	293	38.6
7	284	19.4
8	282	17.6
10	275	19.3
12	235	36.9
14	262	8.4
17	238	19.9
18	284	18.7
20	269	12.7
21	255	19.4
28	219	19.9
33	95	14.8
34	172	18.5
36	106	6.6
37	79	7.8
38	277	49.1
41	58	1.1
42	44	1.6
43	33	5.4
44	26	0.3
45	320	--
46	286	34.2
47	290	65.2
48	313	32.3
49	283	40.4
50	287	12.4

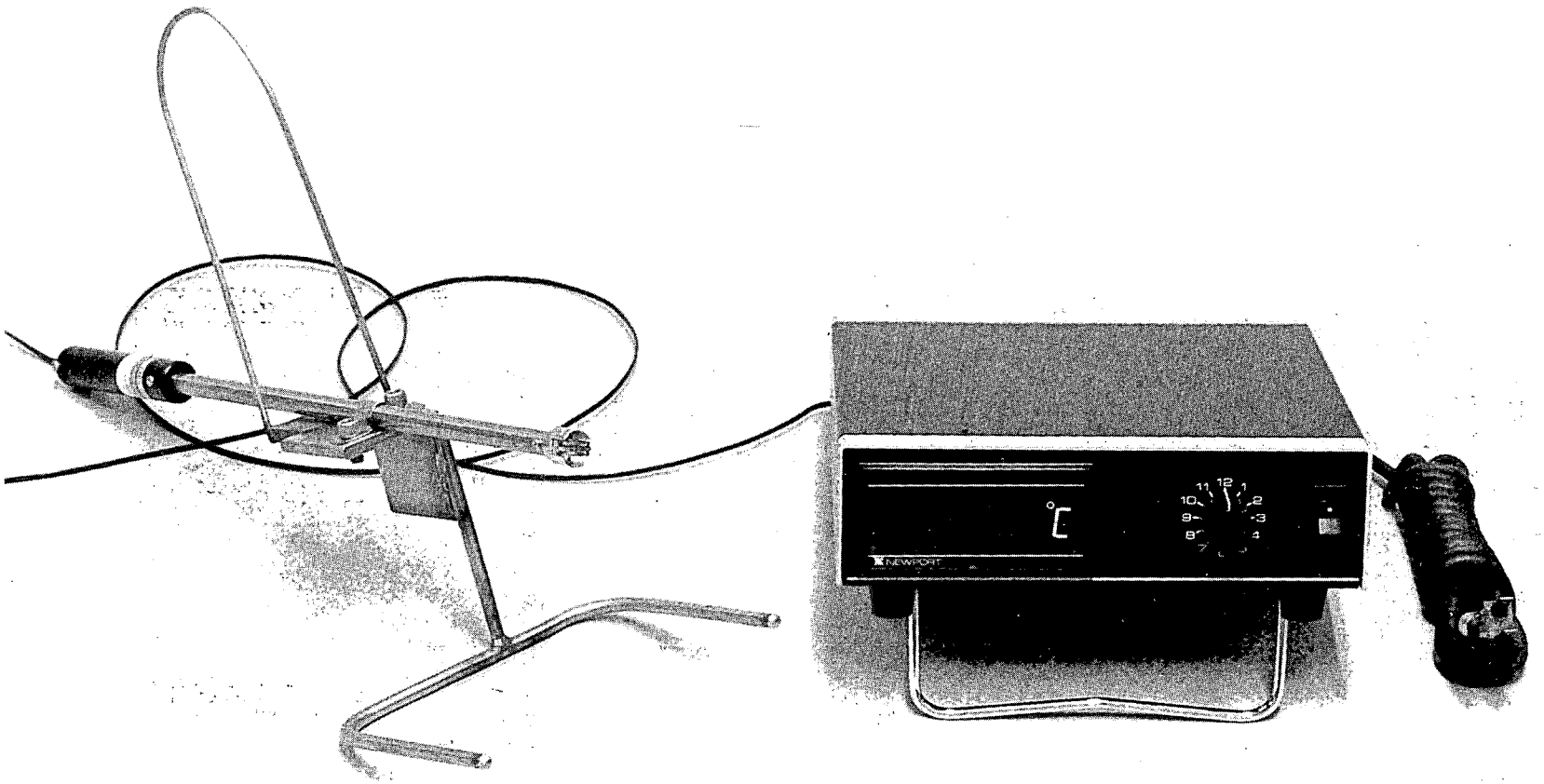

8707264-6cn

FIGURE 6.2. Temperature Probe Equipment System

guide. The temperature probe consists of an Omega surface thermocouple having a flexible stainless steel tip so that little pressure is needed to ensure good contact with the canister. A temperature probe alignment guide was made to hang above the canister, with five pieces of angle steel serving as resting points for the temperature probe. The alignment guide was designed so that the upper position corresponds to the top surface of the glass in the canister and the lower four positions are below the glass surface.

The canisters sat in the air lock for a minimum of 2 hr before the temperature scan was conducted to let them reach thermal steady state. The five temperature measurements obtained using the temperature probe alignment guide for each canister are reported in lines 23-27 of Appendix C. The lid temperature of the canister was also taken and is reported in line 22 of Appendix C. The temperature of the bottom flange was recorded for the last eight canisters and is reported in line 28 of Appendix C. The average of the lower four temperatures, those in the glass section, is reported in line 29 of Appendix C for each canister. Table 6.3 summarizes the canister surface temperature data that are presented in Appendix C. In this table the average temperature, standard deviation, and minimum and maximum values are given for the seven temperatures recorded for each canister as well as the average of the four lower positions on the canister (36, 56, 76 and 96 cm) and the maximum variation of each canister (maximum temperature minus minimum temperature). The average of the lower four temperatures was 171°C, and the

TABLE 6.3 Canister Surface Temperature Summary

Distance from Top of Canister, cm	Average, °C	Standard Deviation, °C	Minimum, °C	Maximum, °C
Lid	89	11	70	118
15	121	16	87	155
36	166	19	128	201
56	172	20	132	207
76	176	18	135	208
96	168	18	123	204
Lower Flange	144	22	105	174
Avg. of Lower Four	171	18	133	205
Max.-Min.	57	12	28	79

average lid temperature was 89°C for the 30 canisters. The maximum average temperature for a canister was 205°C, and the minimum average temperature was 133°C. The average maximum temperature difference was 57°C.

The canister surface temperatures were also analyzed for the individual RLFCM campaigns. The average of the lower four canister surface temperatures was 171°C with a standard deviation of 16°C for RLFCM-7, 159°C with a standard deviation of 18°C for RLFCM-8, and 181°C with a standard deviation of 12°C for RLFCM-9.

6.3 CANISTER WEIGHT MEASUREMENT

The canister weighing system was used to weigh each canister after it was electropolished and rinsed. The weighing system consisted of a Dillon Model Z load cell, lifting bail, Dillon Model SG1000P digital readout, and 15 m of connecting cable. The load cell was connected in series with the 2.4-m lifting yoke before a canister was removed from the RST. The weight of the canister was then recorded after the canister was allowed to dry. The canister weights are shown in line 39 of Appendix C. The individual component weights of the empty canisters (canister, lid, Fiberfrax insulation, and helium capsule) are given in lines 33-36 of Appendix C and the total empty weight of each canister is given in line 37. The amount of metal removed during electropolishing, 1.1 kg, was determined by weighing a canister before and after electropolishing. The weight of glass in each canister, line 40 of Appendix C, was calculated by subtracting the total empty canister weight and the weight of metal removed during electropolishing from the full canister weight. The volume of glass in each canister, line 41 of Appendix C, was calculated based on void space measurements taken prior to welding. The glass specific gravity, line 42 of Appendix C, was calculated by dividing the glass weight by the glass volume for each canister. Table 6.4 summarizes the canister weight data. This table reports the average weight, standard deviation, maximum weight, and minimum weight, as well as the glass volume and specific gravity, for the 30 canisters.

TABLE 6.4. Canister Weight Data Summary

	Average	Standard Deviation	Minimum	Maximum
Canister Weight, kg	73.4	1.1	71.4	76.4
Lid Weight, kg	5.2	0.0	5.1	5.2
Fiberfrax Weight, kg	0.5	0.0	0.5	0.5
Helium Capsule Weight, kg	0.7	0.0	0.7	0.7
Total Empty Canister Weight, kg	79.8	1.1	77.8	82.8
Weight Removed in EPT, kg	1.1	0.0	1.1	1.1
Full Canister Weight, kg	237	6.0	222	249
Glass Weight, kg	158.3	5.9	143.6	171.4
Glass Volume, liters	60.6	1.6	58.6	64.2
Glass Specific Gravity	2.61	0.10	2.32	2.81

6.4 CANISTER STRAIGHTNESS AND OVALITY TEST

One of the quality assurance criteria required by the FRG was that the canisters pass a go/no go test for ovality and straightness. This was necessary so that the canisters will fit in the tubes of the Asse Mine in Germany. The FRG supplied two tubes, one large tube (310 mm inside diameter) and one small tube (306 mm inside diameter), that the canisters were required to fit through. The smaller tube was to be used for each canister. In the event that a canister failed to pass through the small tube, the larger one would be used to determine if the canister was shippable.

The ovality and straightness test consisted of lowering the canister into the tube, which was mounted on the side of the electropolisher rack in A-Cell. The canister was then rotated 180° and raised back out of the tube. All 30 canisters passed through the smaller tube without difficulty; thus, the larger tube was not needed during the A-Cell operations.

6.5 GAMMA SCAN

Gamma scanning of the FRG canisters was performed to determine the homogeneity of ^{137}Cs in the canister glass. Canisters contain ^{90}Sr in addition to ^{137}Cs, but this isotope is difficult to measure since no significant γ-activity is associated with its decay.

Canisters were gamma scanned in the decontamination cell using a GeLi detector which monitored gamma emissions through a field-of-view restricting

collimator. The system depicted in Figure 6.3 was used to draw the canister up out of the canister ovality gauge with the A-Cell crane. The ovality gauge was used to position the canister at a fixed distance from the GeLi detector. As the canister was lifted past the collimator at a fixed rate, the gamma measurements were obtained. Two gamma scans of each canister were obtained at 180° from each other. This second scan was used as a further check of glass homogeneity.

Gamma scanning did not provide absolute γ-detection; however, the gamma system sensitivity was invariant throughout each scan. Therefore, all canister-scan data were collected under similar conditions so that all canister results are comparable.

The three sets of canisters produced contained different levels of ^{137}Cs within the glass. The specifications for the first and third sets of ten

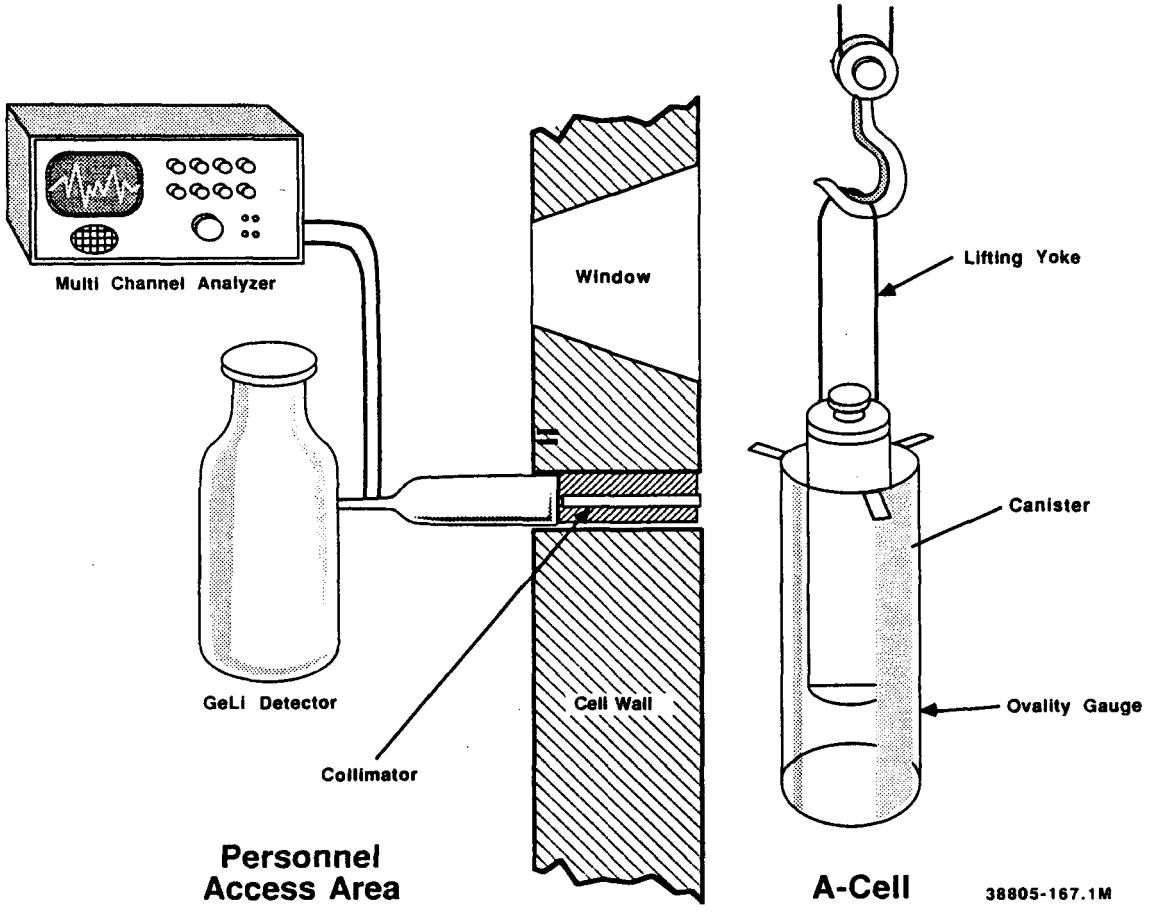

FIGURE 6.3. Gamma Scan System

canisters called for an equal cesium content in each canister. If the glass was homogeneous in ^{137}Cs, the gamma scan would reveal this. Figure 6.4 shows a typical gamma scan from either the first or third sets of canisters. The second set of canisters contained varied amounts of cesium, as explained in Section 2.0 of this report. The cesium concentration in the glass of the first canisters was the same as that of the first set of ten canisters. Gamma scans showed that the cesium concentration gradually decreased throughout production of this set. Figure 6.5 is a typical scan from this set of ten canisters.

Detection of a void within the glass was observed for only one canister (canister no. 33), confirmed by weight measurement. Figure 6.6 shows the gamma scan from this canister, with the area labeled where a void is suspected. There were two glass pours into the canister, one with a higher cesium concentration than the other. If no void were present, the scan for the first pour would not have the lower step labeled void on the figure. It was

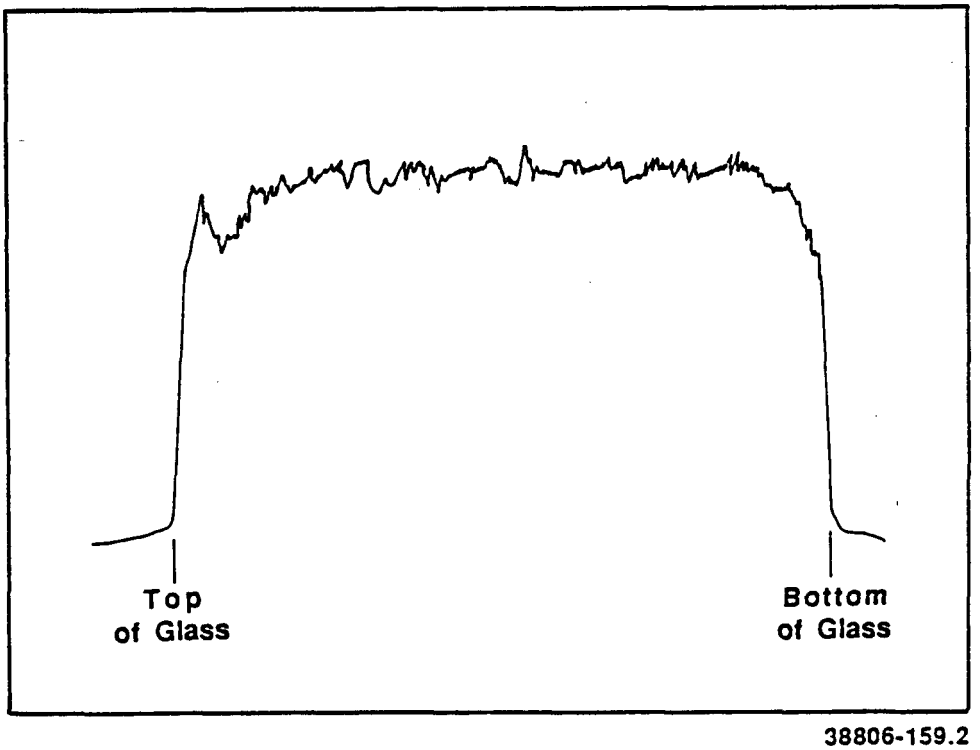

FIGURE 6.4. Gamma Scan of Normal Canister

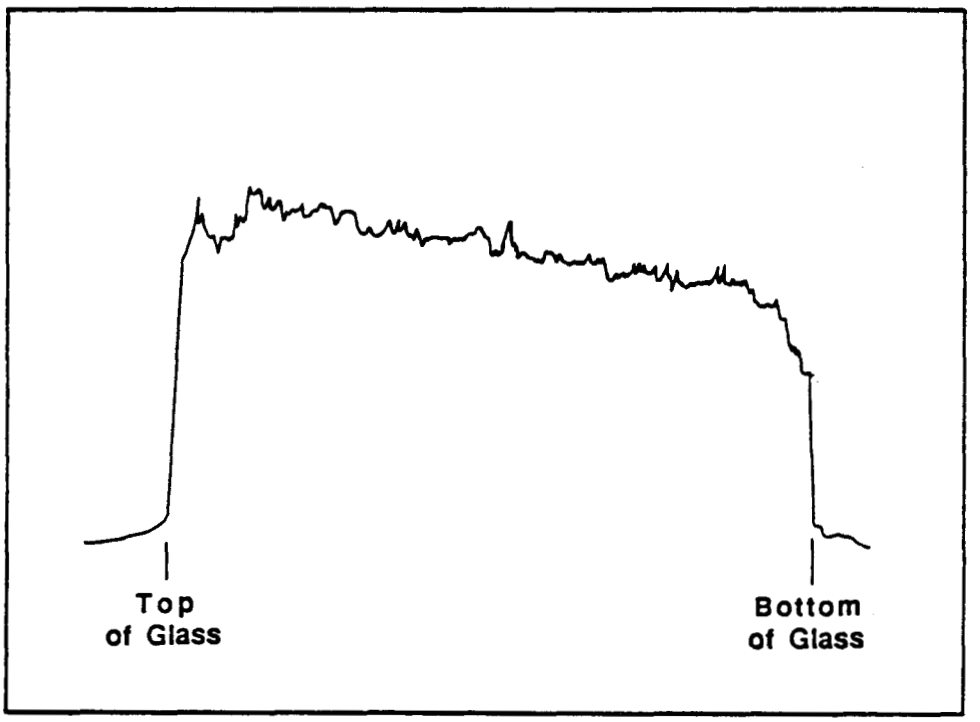

FIGURE 6.5. Typical Gamma Scan of RLFCM-8 Canister

determined from this scan that the void area is ~15 cm long. It is evident that the void area is not completely void of glass since a fairly strong gamma emission from this area was present. The void area probably contains thin strands of hairlike glass.

One further measurement was performed on selected canisters to determine the distribution of gamma energy emitted from the canisters. This measurement was obtained by positioning a stationary canister opposite the collimator and detector and using the multichannel analyzer. A scan from 0 to 1024 MeV was obtained similar to that shown in Figure 6.7. This scan shows that a large portion of the γ-emissions is in the lower energy area of the scan, a phenomenon which is discussed in Section 6.1.

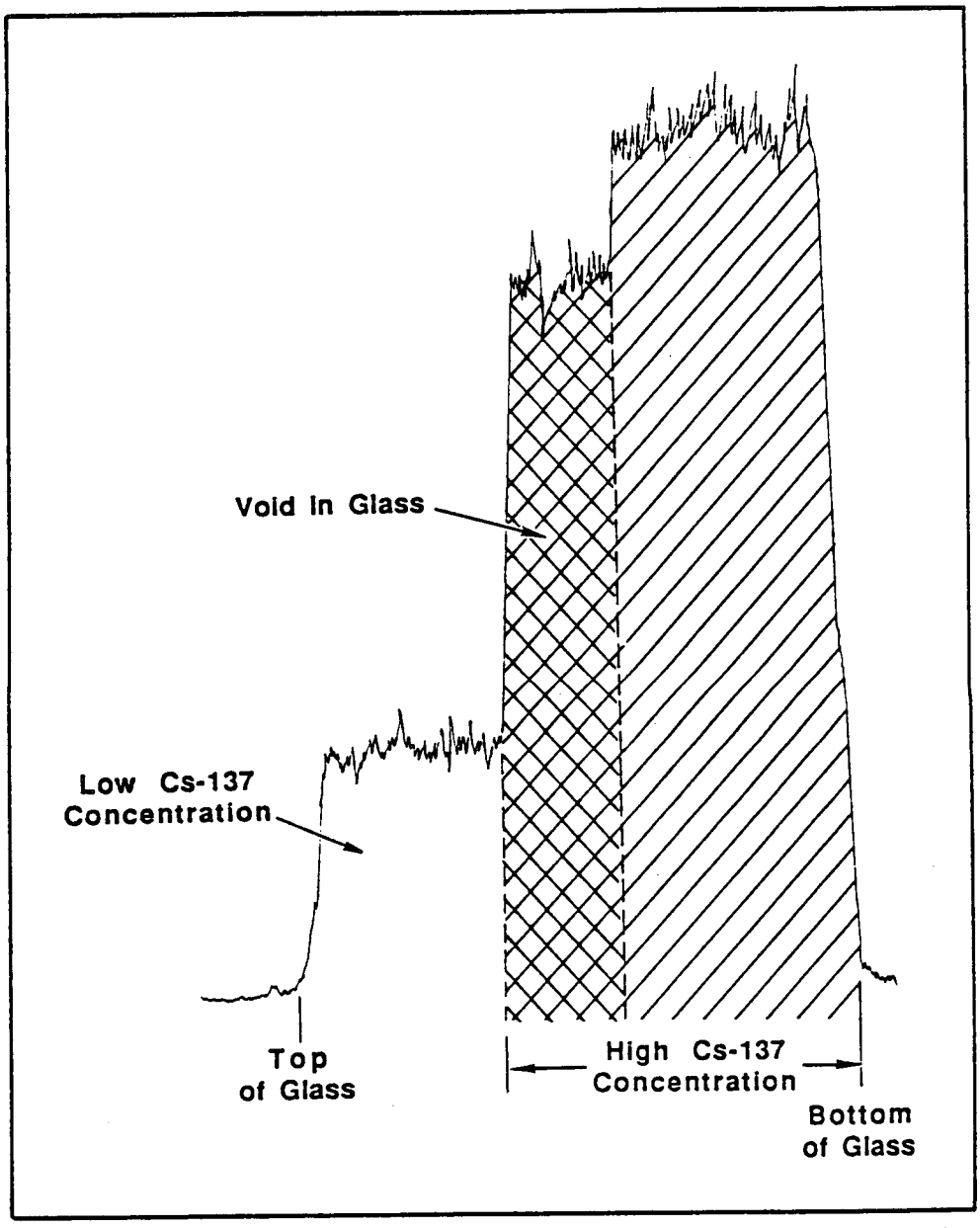

FIGURE 6.6. Gamma Scan of Canister with Void

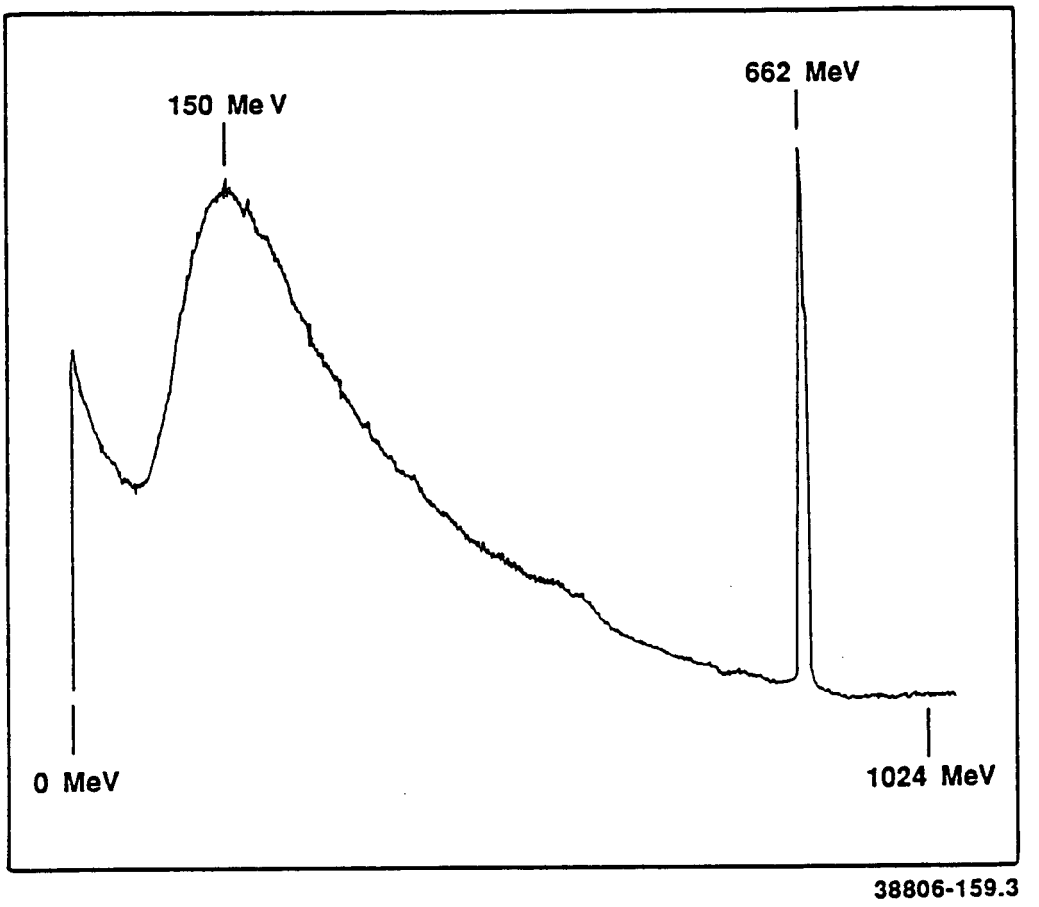

FIGURE 6.7. Gamma Spectrum of RLFCM Glass

7.0 GLOSSARY

°C - degrees centigrade
Am - americium
amp - ampere
atm - atmosphere
Bq - becquerel
cc - cubic centimeter
Ci - curie
cm - centimeter
Co - cobalt
Cs - cesium
ct/min - counts per minute
dc - direct current
DF - decontamination factor
dia - diameter
dpm - disintegrations per minute
EPT - electropolishing tank
FRG - Federal Republic of Germany
g - gram
GLDS - glass-level detection system
GTA - gas tungsten arc
HEDL - Hanford Engineering Development Laboratory
hr - hour
ICP - inductively coupled argon plasma emission spectroscopy
ICP/AES - Inductively Coupled Plasma/Atomic Emission Spectrometer
kCi - kilocurie
kg - kilogram
kPa - kiloPascals
kW - kilowatt
L - liter
μg - microgram
μL - microliter
μm - micrometer
m - meter
min - minute
mL - milliliter
mm - millimeter
PNL - Pacific Northwest Laboratory
ppm - parts per million
R - Roentgen
RLFCM - radioactive liquid-fed ceramic melter
RST - rinse/soak tank
sec - second
Sr - strontium
V - volt
W - watt
WCSR - water-cooled storage rack
wt% - weight percent

APPENDIX A

ESTIMATED CHEMICAL COMPOSITIONS OF THE GLASS WITHIN THE 30 FRG CANISTERS

RLFCM-7 GLASS COMPOSITIONS

ASSUMED OXIDE	1 CAN #1 WT%	2 CAN #2 WT%	3 CAN #3 WT%	4 CAN #5 WT%	5 CAN #6 WT%	6 CAN #7 WT%	7 CAN #8 WT%	8 CAN #12 WT%	9 CAN #17 WT%	10 CAN #14 WT%	AVERAGE RLFCM-7
Al2O3	2.98	2.87	2.90	3.27	2.44	2.69	3.08	2.85	2.86	2.82	2.88
B2O3	10.81	10.98	11.35	13.12	14.46	14.69	14.66	15.34	15.63	15.80	13.68
BaO	1.00	1.08	1.17	0.94	0.76	0.94	1.12	1.11	1.16	1.18	1.05
CaO	2.23	1.91	1.70	1.56	1.35	1.44	1.39	1.23	1.22	1.23	1.52
CeO2	0.00	0.00	0.00	0.00	0.00	0.00	0.00	0.19	0.20	0.24	0.06
Cr2O3	0.66	0.61	0.55	0.53	0.44	0.50	0.60	0.64	0.64	0.63	0.58
Cs2O	4.60	4.78	4.77	5.19	5.11	5.45	5.84	4.90	4.66	4.91	5.02
Fe2O3	11.63	11.11	10.84	8.95	10.55	11.91	12.49	11.98	11.37	11.01	11.18
La2O3	1.18	1.21	1.25	1.13	0.94	0.97	1.00	0.92	0.86	0.92	1.04
Li2O	0.98	0.74	0.52	0.29	0.21	0.13	0.10	0.07	0.05	0.04	0.31
MgO	1.22	1.08	0.92	0.81	0.64	0.68	0.68	0.62	0.61	0.57	0.78
MnO2	0.91	0.93	1.00	0.70	0.58	0.72	0.80	0.81	0.79	0.80	0.80
MoO3	0.12	0.11	0.05	0.03	0.04	0.02	0.00	0.02	0.01	0.08	0.05
Na2O	21.50	20.32	17.93	15.85	13.67	15.50	16.40	14.29	14.88	14.64	16.50
Nd3O3	0.53	0.60	0.72	0.58	0.50	0.61	0.71	0.77	0.75	0.78	0.65
NiO	0.38	0.80	0.44	0.35	0.29	0.33	0.35	0.34	0.31	0.30	0.39
PbO	0.00	0.00	0.00	0.00	0.55	0.51	0.00	0.00	0.31	0.22	0.16
RuO2	0.10	0.07	0.06	0.00	0.00	0.00	0.00	0.00	0.00	0.00	0.02
SiO2	36.67	38.12	41.31	44.53	45.71	41.13	38.76	42.14	42.03	42.07	41.25
SrO	1.65	1.78	1.90	1.72	1.45	1.57	1.69	1.60	1.54	1.57	1.65
TiO2	0.41	0.34	0.27	0.25	0.14	0.10	0.21	0.07	0.05	0.08	0.19
ZnO	0.11	0.21	0.09	0.03	0.05	0.06	0.08	0.05	0.04	0.06	0.08
ZrO2	0.32	0.35	0.25	0.17	0.13	0.05	0.05	0.07	0.05	0.05	0.15
TOTAL	100.00	100.00	100.00	100.00	100.00	100.00	100.00	100.00	100.00	100.00	100.00

RLFCM-8 GLASS COMPOSITIONS

ASSUMED OXIDE	1 CAN #21 WT%	2 CAN #28 WT%	3 CAN #34 WT%	4 CAN #33 WT%	5 CAN #36 WT%	6 CAN #37 WT%	7 CAN #41 WT%	8 CAN #42 WT%	9 CAN #43 WT%	10 CAN #44 WT%	AVERAGE RLFCM-8
Al2O3	2.76	2.63	2.55	2.57	2.37	2.42	2.64	2.52	2.65	2.70	2.58
B2O3	15.51	15.94	14.85	14.77	13.74	13.24	13.58	14.17	15.18	15.51	14.65
BaO	1.13	1.12	1.12	1.10	1.12	1.16	1.12	1.05	1.15	1.18	1.13
CaO	1.27	1.29	1.32	1.35	1.23	1.18	1.14	1.00	1.28	1.42	1.25
CeO2	0.11	0.00	0.09	0.00	0.00	0.20	0.13	0.00	0.00	0.00	0.05
Cr2O3	0.59	0.54	0.47	0.34	0.37	0.36	0.32	0.29	0.24	0.23	0.38
Cs2O	5.08	4.34	3.59	1.59	2.09	1.30	1.03	0.76	0.52	0.48	2.08
Fe2O3	10.92	10.52	9.73	10.20	9.37	9.57	9.74	10.19	10.30	10.45	10.10
La2O3	0.96	0.90	0.85	1.05	1.03	1.37	1.35	1.26	0.98	0.91	1.07
Li2O	0.02	0.00	0.00	0.00	0.00	0.00	0.00	0.00	0.00	0.00	0.00
MgO	0.56	0.56	0.58	0.53	0.49	0.50	0.51	0.47	0.61	0.61	0.54
MnO2	0.81	0.90	0.91	1.31	1.05	1.18	1.36	1.51	1.50	1.53	1.20
MoO3	0.03	0.00	0.00	0.00	0.00	0.00	0.00	0.00	0.00	0.00	0.00
Na2O	14.81	14.35	14.65	12.76	12.36	12.00	11.88	11.52	13.60	14.34	13.22
Nd3O3	0.72	0.62	0.66	0.72	0.62	0.81	0.82	0.76	0.70	0.66	0.71
NiO	0.30	0.29	0.00	0.32	0.28	0.29	0.29	0.35	0.34	0.00	0.25
PbO	0.00	0.00	0.00	0.00	0.00	0.00	0.00	0.00	0.00	0.00	0.00
RuO2	0.00	0.00	0.00	0.00	0.00	0.00	0.00	0.00	0.00	0.00	0.00
SiO2	42.32	43.36	46.00	48.46	50.81	51.40	51.15	51.16	48.27	47.26	48.02
SrO	1.95	2.45	2.52	2.81	2.97	2.95	2.87	2.86	2.63	2.68	2.67
TiO2	0.09	0.12	0.06	0.07	0.07	0.05	0.05	0.07	0.04	0.05	0.07
ZnO	0.03	0.05	0.03	0.00	0.02	0.00	0.00	0.00	0.00	0.00	0.01
ZrO2	0.04	0.03	0.02	0.05	0.03	0.05	0.03	0.07	0.03	0.00	0.04
TOTAL	100.00	100.00	100.00	100.00	100.00	100.00	100.00	100.00	100.00	100.00	100.00

RLFCM-9 GLASS COMPOSITIONS

ASSUMED OXIDE	1 CAN #10 WT%	2 CAN #18 WT%	3 CAN #20 WT%	4 CAN #38 WT%	5 CAN #45 WT%	6 CAN #46 WT%	7 CAN #47 WT%	8 CAN #48 WT%	9 CAN #49 WT%	10 CAN #50 WT%	AVERAGE RLFCM-9
Al2O3	2.38	2.26	2.21	2.12	2.20	2.02	2.14	2.01	2.03	2.28	2.17
B2O3	15.25	15.43	15.53	15.42	14.78	14.19	13.56	14.21	14.94	15.12	14.84
BaO	0.95	0.94	0.98	1.02	1.06	1.04	1.06	1.06	1.06	1.04	1.02
CaO	0.78	0.74	1.01	0.80	0.78	0.73	0.77	0.78	0.76	0.75	0.79
CeO2	0.04	0.06	0.23	0.07	0.06	0.00	0.15	0.00	0.00	0.10	0.07
Cr2O3	0.28	0.30	0.37	0.38	0.38	0.63	0.52	0.47	0.54	0.58	0.45
Cs2O	5.09	5.37	5.33	5.41	5.33	6.11	5.84	6.30	6.38	6.21	5.74
Fe2O3	9.87	9.58	9.61	9.64	9.82	9.88	10.21	10.12	10.23	10.28	9.93
La2O3	1.12	1.23	1.43	1.53	1.63	1.63	1.68	1.71	1.71	1.68	1.53
Li2O	0.00	0.00	0.00	0.00	0.00	0.00	0.00	0.00	0.00	0.00	0.00
MgO	0.44	0.43	0.46	0.43	0.44	0.44	0.44	0.44	0.43	0.43	0.44
MnO2	1.39	1.29	1.22	1.17	1.09	1.04	1.01	0.97	0.95	0.94	1.11
MoO3	0.00	0.00	0.00	0.00	0.00	0.00	0.00	0.00	0.00	0.00	0.00
Na2O	10.51	10.57	10.56	11.35	11.48	11.46	12.25	12.12	12.53	13.00	11.58
Nd3O3	0.71	0.73	0.90	0.82	0.88	0.88	1.06	0.93	0.97	1.05	0.89
NiO	0.45	0.47	0.45	0.42	0.43	0.44	0.44	0.41	0.43	0.42	0.44
PbO	0.00	0.00	0.00	0.00	0.00	0.00	0.00	0.00	0.00	0.00	0.00
RuO2	0.00	0.00	0.00	0.00	0.00	0.00	0.00	0.00	0.00	0.00	0.00
SiO2	47.95	47.89	47.04	46.73	47.04	47.14	46.53	46.34	45.05	44.15	46.59
SrO	2.70	2.60	2.57	2.57	2.52	2.31	2.23	2.05	1.94	1.86	2.34
TiO2	0.04	0.04	0.04	0.03	0.03	0.02	0.03	0.03	0.04	0.03	0.03
ZnO	0.00	0.01	0.00	0.01	0.00	0.00	0.00	0.00	0.00	0.00	0.00
ZrO2	0.05	0.06	0.06	0.05	0.06	0.05	0.07	0.05	0.02	0.06	0.05
TOTAL	100.00	100.00	100.00	100.00	100.00	100.00	100.00	100.00	100.00	100.00	100.00

APPENDIX B

ANALYTICAL METHODS USED TO CHARACTERIZE THE CHEMICAL AND RADIOCHEMICAL COMPOSITION OF THE FRG CANISTERS

APPENDIX B

ANALYTICAL METHODS USED TO CHARACTERIZE THE CHEMICAL AND RADIOCHEMICAL COMPOSITION OF THE FRG CANISTERS

During RLFCM operations, primary process streams, including radioactive feed slurries and product glass streams, were sampled. These samples were transferred to an adjacent cell (C-Cell), where all samples were routinely measured for the integrated gamma intensity of ^{137}Cs. The glass samples were crushed and sized to <100 mesh before gamma measurement. The crushed glass sample and melter feed samples were transferred to the Hanford Engineering Development Laboratory (HEDL) in an adjacent building for fusion dissolution prior to analysis. Dissolved samples were analyzed radiochemically by HEDL and analyzed in an inductively coupled plasma (ICP) apparatus by PNL. These analytical methods are described in the following sections. Figure B.1 is a block diagram showing the steps in processing the analytical samples.

GLASS SLURRY ANALYSES

Slurried feed samples having a volume of ~100 mL were analyzed to verify the composition of the feed formulation. To ensure correct feeding of the RLFCM, these samples were analyzed rapidly on a priority basis. The gamma counting of these samples in C-Cell, before transfer to the fusion dissolution hot cell, allowed the rapid semiquantitative determination of the ^{137}Cs content. Complete analyses, except for ^{90}Sr, require about a 24-hr time period.

After gamma-counting in C-Cell, the feed samples were loaded into a one-ton cask and shipped to a 325 Building hot cell for fusion dissolution, dilution, radiochemical analysis, and ICP analyses.

Fusion Dissolution and Dilution

The fusion dissolution steps for feed slurry samples are as follows:

- homogenize slurry with magnetic stirring bar

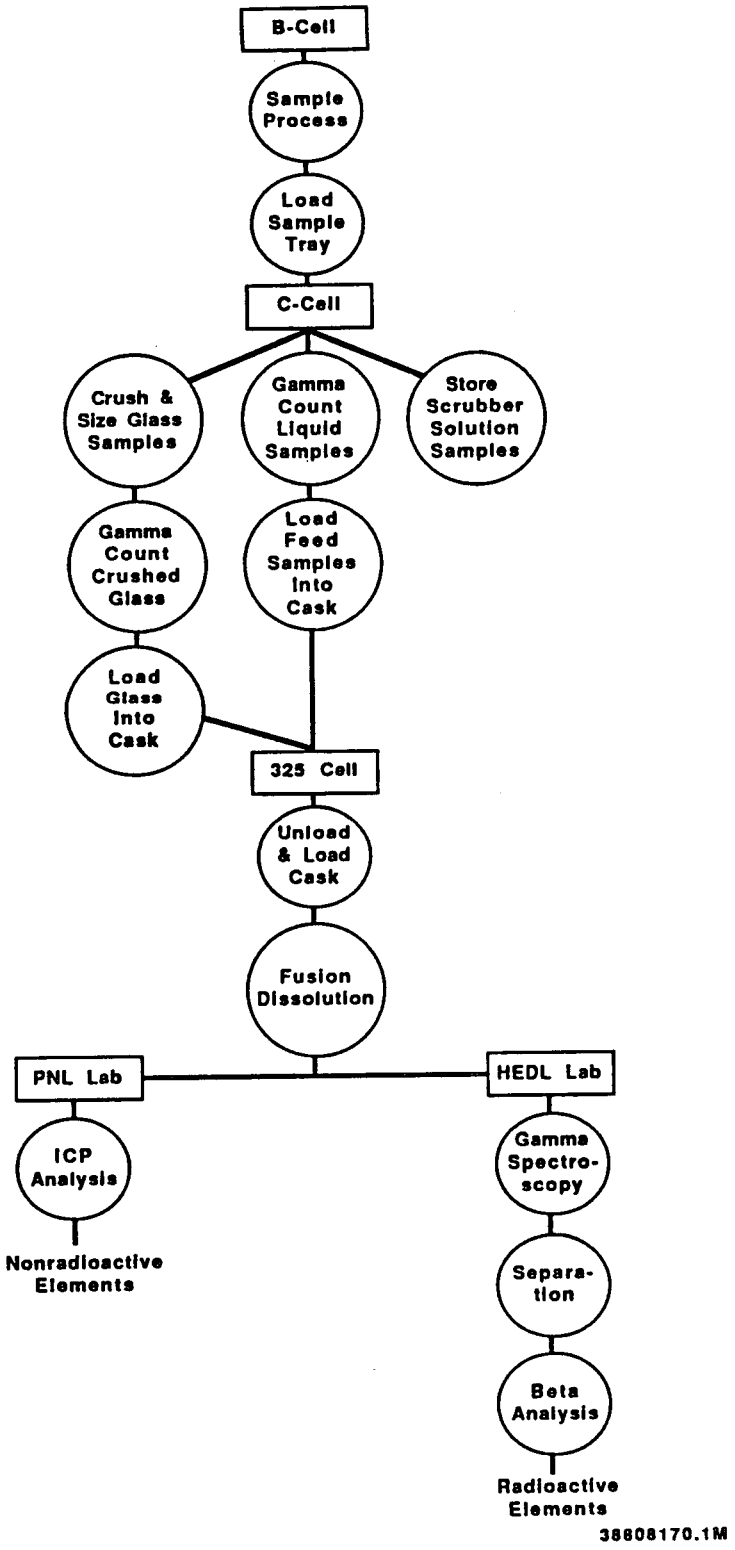

FIGURE B.1. Analytical Sampling Flowsheet

- prepare 1-mL Eppendorf pipette by cutting off tip to prevent plugging
- preweigh one nickel metal crucible and one zirconium metal crucible
- turn off stirrer and take 1-mL sample for each crucible
- reweigh crucible to determine weight of feed sample
- add saturated KOH solution to nickel metal crucible until solution is basic
- add saturated NaOH to zirconium metal crucible until solution is basic
- dry sample under heat lamp
- add 2.5-g KOH and 0.1-g KNO_3 to zirconium crucible
- heat both crucibles slowly to 600°C and hold for 30 minutes
- cool and dissolve in 50 mL of 30% HCl
- if necessary, gently heat solution to aid in dissolving the fused sample
- cool and dilute to volume in a 250-mL volumetric flask with demineralized water
- after mixing, remove 1 mL of solution and make a 10:1 dilution with demineralized water
- send 1 mL of diluted sample to radiochemistry laboratory
- send remainder of diluted sample (9 mL) to ICP laboratory.

Radiochemical Analyses

At the radiochemistry laboratory the ^{137}Cs is analyzed by gamma spectrometry and the ^{90}Sr by cation exchange separation.

Cesium Analysis by Gamma Spectrometry

In gamma spectrometry the abundance of each gamma-emitting isotope is measured by the counts observed as a "peak" at the gamma energies characteristic of each isotope. Counts are converted to disintegrations using the detector efficiency for the specific energy and the gamma abundance for the

specific decay process. For ^{137}Cs measurements the gamma spectrometer consists of a Tracer-Northern TN-4000 with a GeLi detector. The gamma spectrometer is calibrated by generating efficiency curves for each counting position from several National Bureau of Standards gamma standards. This efficiency curve relates gamma counts to actual gamma activity over the energy range of ~40 KeV to 1 MeV, and each efficiency curve is stored in the computer memory of the TN-4000. During data reduction, when a gamma peak is observed, the efficiency is automatically calculated and printed with the net counts observed for each peak.

The daily control standard for the TN-4000 is a mixture of ^{241}Am, ^{137}Cs, and ^{60}Co. This standard is encapsulated to maintain a constant and reproducible geometry. Limits are determined by counting the standard several times and calculating the average counts and statistical limits for each system. The following two-step daily control count was done at the beginning of each shift.

Step 1 - Adjust gain and zero, as required, with the daily control standard using the appropriate daily control and energy calibration guide.

Step 2 - Count the daily standard for 600 seconds and record counts on the appropriate control chart. Counts must be within limits before samples may be counted.

The following is the sample counting procedure:

Step 1 - While the TN-4000 is in ACQUIRE mode, place the prepared sample on one of the counting positions on the GeLi detector; observe the dead time on the dead-time meter (a counting position must be selected to give a dead time of <10%).

Step 2 - Dilute sample volume to 10 $\pm$0.1 mL and mix in a 15-mL screw-cap vial to conform to the geometry used in calibrating the gamma spectrometry system.

Step 3 - Stop the ACQUIRE mode, clear the memory, and restart the ACQUIRE mode. Sample counting times may vary from 10 to 60 min, depending on the activity level of the sample.

Step 4 - Using the appropriate file in the computer memory, perform the peak search and automatic calculation for the isotopes observed. If an observed isotope is not calculated automatically, manually calculate its abundance using the following equation:

$$A = \frac{(B)(C)(D)}{(E)(F)}$$

where

A = dis/min/mL of observed peak
B = net counts in "peak"
C = volume factor to relate to 1 mL
D = efficiency as γ/ct
E = minutes counted
F = γ/dis in decay scheme expressed as a decimal fraction.

Strontium Analysis by Cation Exchange Separation

In this method the ^{90}Sr is separated from other radioactive species by selective elution from a cation exchange resin using 2-methyllactic acid. Following separation, the growth of ^{90}Y is measured by beta counting. The ^{90}Sr is then calculated based on the growth of the ^{90}Y daughter over a measured period of time. The technique of Roberts (1961) is used.

The procedure is as follows:

Step 1 - Prepare a 300 ($\pm$20) μL column of AG-50W,® X-8, 200 to 400 mesh, NH_4^+ form, ion-exchange resin.

® AG-50W is a registered trademark of Bio-Rad Laboratories, Richmond, CA.

Step 2 - To the column, accurately add up to 500 (±10) μL of test solution. Record the volume used on the Analytical Report (Form 54-7340-015).

Step 3 - Wash the resin column with 500 (±10) μL of deionized water.

Step 4 - Wash the resin column with three 1 (±0.01) mL portions of 0.2M hydrofluoric acid.

Step 5 - Wash the resin column with four 1 (±0.01) mL portions of 0.7M methyllactic acid.

Step 6 - Elute strontium with 3.5 (±0.2) mL of 1.0M methyllactic acid; collect the effluent in a 2-dram vial containing 400 (±10) μL of 8M nitric acid.

Step 7 - Mix the solution in the 2-dram vial and transfer the solution to a fresh 300-μL column of AG-50W, X-8, 200 to 400 mesh, NH_4^+ form, ion-exchange resin.

Step 8 - Wash the 2-dram vial with three 1 (±0.01) mL portions of deionized water and transfer the washes to the resin column.

Step 9 - Wash the resin column with three 1 (±0.01) mL portions of 0.7M methyllactic acid. Record time (T_0) and date that the last drop leaves the column on the Analytical Report.

Step 10 - Elute the strontium with 3.5 (±0.05) mL of 1.0M methyllactic acid. Collect in a 10-mL volumetric flask.

Step 11 - Dilute the solution in the volumetric flask to 10 mL using deionized water. Add a stirring bar and stir thoroughly.

Step 12 - Accurately pipette the volume required onto a stainless steel beta-counting disc. Record volume on the Analytical Report.

Step 13 - Dry under a heat lamp until completely dry.

Step 14 - Immediately count the beta activity on the disc for 10 min using the Beta Counting (HTA-4-8) procedure. Record time (T_1) and date that the count is started on the Analytical Report.

Step 15 - Recount the beta disc in 3 to 4 days for 10 min. Record time (T_2) and date that the count is started on the Analytical Report.

Step 16 - Calculate the ^{90}Y counts at equilibrium using the equation:

$$Y = \frac{A - B}{C - D}$$

where $Y = {}^{90}Y$ equilibrium count rate (ct/min)

A = (ct/min-bkgd) at T_2

B = (ct/min-bkgd) at T_1

$$C = e - \frac{Ln2 \times (\Delta T_1)}{64}$$, ΔT_1 is time elapsed from T_0 to T_1 in hours

$$D = e - \frac{Ln2 \times (\Delta T_2)}{64}$$, ΔT_2 is time elapsed from T_0 to T_2 in hours

Step 17 - Calculate the ^{90}Sr disintegrations per minute per milliliter (dis/min/mL) using the following equation. Record the calculation results on the Analytical Report.

$$S = Y \times D \times V$$

where $V = \frac{1}{V_A} \times 10 \times \frac{1}{V_B}$

S = ^{90}Y (dis/min/mL)
Y = ^{90}Y equilibrium count rate from Step 16 (ct/min)
D = disintegrations per count factor for ^{90}Y
V = volume correction factor to correct activity to 1 mL
V_A = volume of sample from step 2 (mL)
V_B = volume of sample pipetted into counting disc in step 12 (mL)
10 = volume from step 11 (mL).

ICP Analysis

The ICP is a spatially stable, chemically inert argon plasma formed by interaction of a radio frequency field and an ionized argon gas stream. An argon carrier gas aspirates the liquid sample into the spray chamber and transports the smaller sample droplets into the plasma. The high temperature (about 10,000°K) in the plasma desolvates the droplets and dissociates the sample material into individual atoms and ions, which are excited to emit light at wavelengths characteristic of the elements in the sample. A photomultiplier tube-spectrometer measures the intensity of each spectral line. The digitalized electrical signals are converted by the computer into mg/L (μg/mL) units, which are printed directly onto the input/output terminal.

The analyzer is an Applied Research Laboratory Model 3580 Inductively Coupled Plasma/Atomic Emission Spectrometer (ICP/AES) dedicated to the analysis of radioactive aqueous solutions. A PDP-1103 computer with a Winchester and a floppy disk drive is an integral part of the analyzing system and is used to control the system during acquisition of data, calibration of the system, computation of the results, and management/storage of data.

When the ICP is started, the scanner is calibrated and the spectrometer is profiled. The procedure for analyzing samples is as follows:

- Select a previously established program.
- Select a previously established calibration curve.
- Run the previously selected calibration standards.

- Establish an initial normalization calibration curve to correct for instrument drift.
- Begin sample analyses. During analysis of a series of samples, run at least one of the calibration standards periodically (usually after 5 or 6 samples) to ascertain that the system is still in calibration.

Liquid samples are reported in milligrams per liter. If a dilution is made on liquid samples in the laboratory, the final reported element concentrations are corrected for the dilution. For solid samples, a computer program is used to convert the concentration of each element analyzed by ICP to a wt% element and a wt% oxide.

GLASS ANALYSES

The analyses of the glass poured into the canister were needed to verify that the canisters filled with isotopic heat and radiation sources meet the specifications of the Federal Republic of Germany. Glass samples were taken during each glass pour into the canisters. These glass samples were transferred to C-Cell, where they were crushed, sized, and gamma-counted. A 0.5-g sample of gamma-counted glass was then weighed out and shipped to the 325 Building for fusion-dissolution, radiochemical analyses, and ICP analyses.

Glass fragments were crushed in a stainless steel die-and-punch assembly. This assembly was placed between the platens of a hydraulic press and subjected to a compressive force of about 10,000 pounds for a few seconds, and then the pressure was released. After three pressure cycles, the punch was removed from the die, the compacted mass of crushed glass was stirred, and the punch was reinserted into the die. The three pressurization cycles and glass stirring cycles were repeated three times. After completion of these crush-stirring cycles, the powdered glass was placed into a stainless steel, 100-mesh sieve, and gently tapped. The glass powder passing through the 100-mesh sieve was placed into a 15-mL vial. A 1/2-g sample of the crushed, sieved and gamma-counted glass is weighed, packaged, and shipped to the 325 Building. The sample is dissolved by alkaline-fusion, and radiochemically and ICP analyzed. These steps are identical to those described for the glass slurry analyses.

APPENDIX C

SUMMARY OF FRG CANISTER CHARACTERISTICS AND PRODUCTION DATA

1	Sequence Number	1	2	3	4	5	6
2	Canister Number	2	49	48	12	50	47
3	Date Filled	2/4/86	3/21/87	3/18/87	10/20/86	3/22/87	3/17/87
4	Date Welded	2/17/88	2/17/88	2/18/88	2/22/88	2/23/88	2/24/88
5	Date Leak Checked	2/18/88	2/18/88	2/19/88	2/23/88	2/24/88	2/25/88
6	Date Electropolished	2/18/88	2/19/88	2/22/88	2/23/88	2/24/88	2/26/88
	Time in Turntable (hr)	57.5	65.8	36.1	17.3	23.1	48.9
	Time in Insulated Cooling Pod (hr)	36.5	23.1	65.8	26.8	73.7	29.4
7	Void Height (cm)	15.2	19.3	14.0	8.6	17.1	17.5
8	Helium Capsule Number	05-357	05-462	05-470	05-463	05-466	05-529
9	1 atm pressure (atm)	1.00	0.99	0.98	0.97	0.97	0.96
10	1 atm leak rate (atm cc/sec)	0.0013	0.0023	0.0031	0.0006	0.0019	0.0017
11	Fill Pressure (atm)	50.9	61.2	45.9	24.3	55.3	60.7
12	Pressurized Leak Rate (atm cc/sec)	2.0	4.5	3.2	0.8	4.4	3.5
13	Crimp Time	847	1440	1417	1018	1535	1051
14	Placement Time	1012	1456	1438	1034	1555	1120
15	Weld Time	1046	1530	1510	1121	1623	1156
16	Leak Detection Time	1057	1510	1505	1050	1210	1400
17	Leak Detector Sensitivity (1E-10 atm cc/sec unit)	6.7	6.7	3.4	3.5	3.6	3.8
18	Vessel Background (1E-8 atm cc/sec	1.4	1.4	0.5	0.2	0.3	0.8
19	Gross Leak Rate (1E-8 atm cc/sec)	2.7	1.6	0.6	2.6	0.5	0.4
20	Net Leak Rate (1E-8 atm cc/sec)	1.3	0.2	0.1	2.4	0.3	-0.4
21	Measured Dose Rate (1E3 R/hr)	280	310	340	250	330	320
	Surface Temperatures (C)						
22	Lid		86	93	92	89	96
23	Top Position	140	111	145	127	118	113
24	Second Position	195	163	196	150	184	167
25	Third Position	200	170	195	156	185	171
26	Fourth Position	197	176	193	168	186	180
27	Bottom Position	187	160	188	164	174	192
28	Lower Flange						
29	Average of Four	195	167	193	160	182	177
	Leak Calculations						
30	Void Pressure (atm)	0.7	0.8	0.9	0.9	0.8	0.9
31	Capsule Pressure (atm)	3.0	2.0	1.6	2.3	2.2	2.4
32	Equivalent Leak Rate (1E-8 atm cc/sec)	1.3	0.2	0.1	2.0	0.3	0.0
	Empty Weights						
33	Canister (KG)	73.4	73.6	73.6	72.8	75.8	74.6
34	Lid (KG)	5.2	5.2	5.2	5.1	5.2	5.1
35	Fiberfrax (KG)	0.5	0.5	0.5	0.5	0.5	0.5
36	He Capsule (KG)	0.7	0.7	0.7	0.7	0.7	0.7
37	TOTAL WEIGHT (KG)	79.8	80.0	80.0	79.2	82.2	80.9
	Removal						
38	Electropolishing (KG)	1.1	1.1	1.1	1.1	1.1	1.1
39	Full Canister Weight (KG)	245.4	233.1	243.6	249.5	236.3	240.9
40	Glass Mass (KG)	166.7	154.3	164.7	171.4	155.3	161.1
41	Glass Volume (Liters)	59.3	61.0	62.9	63.1	59.8	59.3
42	Approximate Specific Gravity	2.81	2.53	2.62	2.72	2.60	2.72
	Smears						
43	Beta + Gamma (d/M/100 cm^2)	862	117	1591	LESS THAN DETECTIBLE	LESS THAN DETECTIBLE	222
44	Alpha (d/M/100 cm^2)	-	-	-	-	-	-
45	Cs-137 Concentration (Ci/Kg)	1165	1432	1417	1150	1426	1315
46	Total kCi	196	221	233	197	221	212
47	Sr-90 Concentration (Ci/Kg)	656	667	731	451	677	785
48	Total kCi	110	103	120	77	105	126
49	Decay Heat (Watts)	1664	1747	1924	1462	1765	1862

1 Sequence Number	7	8	9	10	11	12
2 Canister Number	45	38	46	18	28	36
3 Date Filled	3/13/87	3/10/87	3/15/87	3/7/87	12/18/86	1/25/87
4 Date Welded	2/25/88	3/3/88	3/4/88	3/7/88	3/8/88	3/9/88
5 Date Leak Checked	2/26/88	3/4/88	3/5/88	3/8/88	3/9/88	3/10/88
6 Date Electropolished	3/1/88	3/7/88	3/8/88	3/9/88	3/10/88	3/11/88
Time in Turntable (hr)	62.6	42.9	45.4	29.8	24.6	38.4
Time in Insulated Cooling Pod (hr)	45.0	62.6	49.9	21.4	20.5	36.2
7 Void Height (cm)	17.1	16.5	18.2	16.5	10.2	10.2
8 Helium Capsule Number	05-472	05-528	05-535	05-530	05-534	05-542
9 1 atm pressure (atm)	0.91	0.93	0.94	0.94	0.96	0.95
10 1 atm leak rate (atm cc/sec)	0.0020	0.0017	0.0019	0.0024	0.0017	0.0018
11 Fill Pressure (atm)	58.6	56.0	61.2	55.8	30.6	32.3
12 Pressurized Leak Rate (atm cc/sec)	4.0	3.8	4.0	3.8	1.3	1.3
13 Crimp Time	635	1026	955	1244	958	835
14 Placement Time	658	1104	1016	1305	1018	851
15 Weld Time	735	1142	1056	1343	1048	920
16 Leak Detection Time	1655	1135	900	1300	1753	1130
17 Leak Detector Sensitivity (1E-10 atm cc/sec unit)	8.1	4.4	2.8	4.0	4.9	4.3
18 Vessel Background (1E-8 atm cc/sec	0.5	0.0	0.2	5.3	6.6	5.8
19 Gross Leak Rate (1E-8 atm cc/sec)	0.3	0.0	0.4	5.6	5.6	5.6
20 Net Leak Rate (1E-8 atm cc/sec)	-0.2	-0.0	0.2	0.3	-1.0	-0.2
21 Measured Dose Rate (1E3 R/hr)	320	290	300	320	230	110
Surface Temperatures (C)						
22 Lid	103	86	93	89	118	106
23 Top Position	121	117	126	124	151	155
24 Second Position	167	163	183	173	189	181
25 Third Position	168	171	192	177	195	182
26 Fourth Position	163	174	192	187	195	183
27 Bottom Position	156	166	178	184	176	166
28 Lower Flange						
29 Average of Four	163	169	186	180	189	178
Leak Calculations						
30 Void Pressure (atm)	0.9	0.8	0.8	0.8	1.0	1.1
31 Capsule Pressure (atm)	1.5	2.1	2.4	2.0	1.7	2.0
32 Equivalent Leak Rate (1E-8 atm cc/sec)	0.0	0.0	0.2	0.2	0.0	0.0
Empty Weights						
33 Canister (KG)	73.4	73.4	73.0	72.4	72.2	73.1
34 Lid (KG)	5.1	5.2	5.1	5.2	5.2	5.2
35 Fiberfrax (KG)	0.5	0.5	0.5	0.5	0.5	0.5
36 He Capsule (KG)	0.7	0.7	0.7	0.7	0.7	0.7
37 TOTAL WEIGHT (KG)	79.7	79.8	79.3	78.8	78.6	79.5
Removal						
38 Electropolishing (KG)	1.1	1.1	1.1	1.1	1.1	1.1
39 Full Canister Weight (KG)	237.2	238.1	235.0	237.2	243.1	240.9
40 Glass Mass (KG)	158.6	159.5	156.8	159.5	165.7	162.5
41 Glass Volume (Liters)	59.7	59.3	59.1	60.2	64.2	64.2
42 Approximate Specific Gravity	2.66	2.69	2.65	2.65	2.58	2.53
Smears						
43 Beta + Gamma (d/M/100 cm^2)	222	213	LESS THAN DETECTIBLE	70	182	
44 Alpha (d/M/100 cm^2)	-	-	-	-	-	-
45 Cs-137 Concentration (Ci/Kg)	1202	1242	1380	1237	1024	455
46 Total kCi	191	198	216	197	170	80
47 Sr-90 Concentration (Ci/Kg)	864	895	880	898	787	975
48 Total kCi	137	143	138	143	130	158
49 Decay Heat (Watts)	1832	1905	1961	1906	1687	1417

1	Sequence Number	13	14	15	16	17	18
2	Canister Number	34	21	14	17	3	44
3	Date Filled	12/19/86	12/17/86	10/23/86	10/21/86	2/5/86	2/1/86
4	Date Welded	3/9/88	3/10/88	3/14/88	3/15/88	3/16/88	3/17/88
5	Date Leak Checked	3/11/88	3/11/88	3/15/88	3/16/88	3/17/88	3/18/88
6	Date Electropolished	3/14/88	3/15/88	3/16/88	3/17/88	3/18/88	3/21/88
	Time in Turntable (hr)	20.8	1315.4	26.9	33.7	36.7	20.0
	Time in Insulated Cooling Pod (hr)	27.8	22.2	35.2	19.0	42.2	24.8
7	Void Height (cm)	11.1	16.5	16.5	16.5	17.8	19.1
8	Helium Capsule Number	05-476	05-547	05-544	05-460	05-208	05-546
9	1 atm pressure (atm)	0.99	0.96	0.97	0.94	1.04	0.92
10	1 atm leak rate (atm cc/sec)	0.0017	0.0020	0.0022	0.0034	0.0025	0.0020
11	Fill Pressure (atm)	36.1	56.0	54.9	54.4	61.0	60.9
12	Pressurized Leak Rate (atm cc/sec)	1.2	3.8	4.0	4.0	3.7	3.6
13	Crimp Time	1350	1322	1401	1024	911	1357
14	Placement Time	1420	1333	1421	1037	947	1408
15	Weld Time	1512	1625	1519	1119	1033	1438
16	Leak Detection Time	1250	1515	1540	1245	1055	1100
17	Leak Detector Sensitivity (1E-10 atm cc/sec unit)	5.5	5.5	4.8	4.3	4.6	4.0
18	Vessel Background (1E-8 atm cc/sec	0.5	0.5	0.1	0.1	0.3	0.2
19	Gross Leak Rate (1E-8 atm cc/sec)	0.4	0.3	0.2	0.4	0.3	0.3
20	Net Leak Rate (1E-8 atm cc/sec)	-0.1	-0.2	0.1	0.3	0.0	0.2
21	Measured Dose Rate (1E3 R/hr)	170	270	270	250	240	26
	Surface Temperatures (C)						
22	Lid	98	76	76	82	81	76
23	Top Position	143	100	95	104	113	87
24	Second Position	158	145	133	149	172	128
25	Third Position	166	151	134	161	176	140
26	Fourth Position	178	157	139	167	178	144
27	Bottom Position	163	149	130	161	168	148
28	Lower Flange						
29	Average of Four	166	151	134	159	173	140
	Leak Calculations						
30	Void Pressure (atm)	1.0	0.4	0.7	0.8	0.8	1.0
31	Capsule Pressure (atm)	1.5	1.8	1.8	1.5	2.2	2.8
32	Equivalent Leak Rate (1E-8 atm cc/sec)	0.0	0.0	0.1	0.3	0.0	0.1
	Empty Weights						
33	Canister (KG)	72.4	72.9	73.4	72.9	71.4	74.3
34	Lid (KG)	5.2	5.2	5.1	5.1	5.2	5.2
35	Fiberfrax (KG)	0.5	0.5	0.5	0.5	0.5	0.5
36	He Capsule (KG)	0.7	0.7	0.7	0.7	0.7	0.7
37	TOTAL WEIGHT (KG)	78.8	79.3	79.7	79.3	77.8	80.6
	Removal						
38	Electropolishing (KG)	1.1	1.1	1.1	1.1	1.1	1.1
39	Full Canister Weight (KG)	240.9	231.3	235.0	235.4	235.4	231.8
40	Glass Mass (KG)	163.2	153.2	156.4	157.3	158.7	152.3
41	Glass Volume (Liters)	63.6	60.2	60.6	60.6	59.4	58.6
42	Approximate Specific Gravity	2.57	2.54	2.58	2.60	2.67	2.60
	Smears						
43	Beta • Gamma (d/M/100 cm^2)	LESS THAN DETECTIBLE	*	60	200	40	70
44	Alpha (d/M/100 cm^2)	-	-	-	-	-	-
45	Cs-137 Concentration (Ci/Kg)	838	1221	1212	1129	1103	110
46	Total kCi	137	187	190	178	175	17
47	Sr-90 Concentration (Ci/Kg)	900	588	450	426	623	955
48	Total kCi	147	90	70	67	99	145
49	Decay Heat (Watts)	1640	1499	1380	1299	1500	1056

1 Sequence Number	19	20	21	22	23	24
2 Canister Number	6	33	1	8	20	10
3 Date Filled	9/30/86	1/30/87	2/1/86	10/19/86	3/8/87	3/6/87
4 Date Welded	3/17/88	3/21/88	3/21/88	3/22/88	3/23/88	3/23/88
5 Date Leak Checked	3/18/88	3/22/88	3/22/88	3/24/88	3/24/88	3/24/88
6 Date Electropolished	3/22/88	3/23/88	3/24/88	3/25/88	3/28/88	3/29/88
Time in Turntable (hr)	78.0	84.8	294.3	24.5	23.6	107.6
Time in Insulated Cooling Pod (hr)	99.5	39.6	50.9	18.0	34.4	27.0
7 Void Height (cm)	19.1	14.0	15.2	17.8	17.2	17.2
8 Helium Capsule Number	05-517	05-548	05-552	05-545	05-554	05-555
9 1 atm pressure (atm)	0.99	1.00	0.98	1.01	0.95	1.05
10 1 atm leak rate (atm cc/sec)	0.0018	0.0027	0.0023	0.0017	0.0021	0.0020
11 Fill Pressure (atm)	60.9	46.7	52.8	61.3	60.0	60.0
12 Pressurized Leak Rate (atm cc/sec)	3.9	1.6	2.9	3.4	3.6	3.0
13 Crimp Time	929	938	1300	1314	809	1314
14 Placement Time	942	1018	1320	1336	815	1334
15 Weld Time	1027	1040	1347	1421	859	1420
16 Leak Detection Time	1310	1354	1612	1051	1248	1457
17 Leak Detector Sensitivity (1E-10 atm cc/sec unit)	4.0	5.5	5.5	5.8	5.8	5.8
18 Vessel Background (1E-8 atm cc/sec	0.2	0.4	0.4	0.2	0.2	0.2
19 Gross Leak Rate (1E-8 atm cc/sec)	0.2	0.6	0.8	0.9	1.2	0.5
20 Net Leak Rate (1E-8 atm cc/sec)	0.0	0.1	0.4	0.6	1.0	0.2
21 Measured Dose Rate (1E3 R/hr)	310	95	250	290	280	290
Surface Temperatures (C)						
22 Lid	83	77	85	89	95	101
23 Top Position	113	117	130	125	134	142
24 Second Position	163	149	166	171	186	201
25 Third Position	182	132	179	182	190	207
26 Fourth Position	181	152	190	186	190	208
27 Bottom Position	173	162	182	164	201	204
28 Lower Flange					165	174
29 Average of Four	175	149	179	176	192	205
Leak Calculations						
30 Void Pressure (atm)	0.8	1.1	1.1	0.9	1.0	1.0
31 Capsule Pressure (atm)	2.1	2.4	2.1	1.6	2.1	2.7
32 Equivalent Leak Rate (1E-8 atm cc/sec)	0.0	0.1	0.3	0.5	0.7	0.2
Empty Weights						
33 Canister (KG)	72.9	73.4	73.4	73.1	73.0	72.5
34 Lid (KG)	5.1	5.2	5.1	5.2	5.2	5.1
35 Fiberfrax (KG)	0.5	0.5	0.5	0.5	0.5	0.5
36 He Capsule (KG)	0.7	0.7	0.7	0.7	0.7	0.7
37 TOTAL WEIGHT (KG)	79.3	79.8	79.8	79.5	79.4	78.8
Removal						
38 Electropolishing (KG)	1.1	1.1	1.1	1.1	1.1	1.1
39 Full Canister Weight (KG)	231.3	222.3	247.7	241.8	236.8	236.8
40 Glass Mass (KG)	153.2	143.6	169.0	163.4	158.5	159.1
41 Glass Volume (Liters)	59.3	61.8	60.9	59.4	59.8	59.8
42 Approximate Specific Gravity	2.58	2.32	2.78	2.75	2.65	2.66
Smears						
43 Beta + Gamma (d/M/100 cm^2)	147	160	89	227	LESS THAN DETECTIBLE	5
44 Alpha (d/M/100 cm^2)	-	-	-	-	-	-
45 Cs-137 Concentration (Ci/Kg)	1290	387	1125	1450	1222	1146
46 Total kCi	198	55	190	237	194	182
47 Sr-90 Concentration (Ci/Kg)	490	1020	590	537	893	894
48 Total kCi	75	146	100	88	142	148
49 Decay Heat (Watts)	1449	1248	1579	1723	1877	1827

1 Sequence Number	25	26	27	28	29	30
2 Canister Number	5	42	43	7	41	37
3 Date Filled	9/29/86	1/29/87	1/31/87	10/9/86	1/28/87	1/27/87
4 Date Welded	3/28/88	3/29/88	3/29/88	3/30/88	3/31/88	3/31/88
5 Date Leak Checked	3/29/88	3/30/88	3/30/88	3/31/88	4/1/88	4/1/88
6 Date Electropolished	3/30/88	3/31/88	4/1/88	4/4/88	4/5/88	4/6/88
Time in Turntable (hr)	63.0	28.6	28.4	76.9	32.3	39.4
Time in Insulated Cooling Pod (hr)	70.5	34.6	19.9	246.5	24.5	30.0
7 Void Height (cm)	17.2	16.5	16.5	19.1	14.0	19.1
8 Helium Capsule Number	05-549	05-567	05-568	05-560	05-566	05-569
9 1 atm pressure (atm)	1.01	1.10	0.99	1.06	0.93	0.92
10 1 atm leak rate (atm cc/sec)	0.0019	0.0019	0.0015	0.0019	0.0013	0.0016
11 Fill Pressure (atm)	60.0	57.6	56.1	61.3	47.5	61.1
12 Pressurized Leak Rate (atm cc/sec)	3.2	2.8	2.7	1.6	1.9	2.9
13 Crimp Time	1300	1315	0933	1300	852	1325
14 Placement Time	1335	1335	0955	1342	913	1337
15 Weld Time	1410	1416	1046	1436	956	1425
16 Leak Detection Time	1422	1442	1235	1258	1110	1300
17 Leak Detector Sensitivity (1E-10 atm cc/sec unit)	5.7	4.4	4.4	4.7	5.1	5.1
18 Vessel Background (1E-8 atm cc/sec	0.1	0.2	0.2	0.2	0.2	0.2
19 Gross Leak Rate (1E-8 atm cc/sec)	0.2	0.5	0.2	0.2	0.8	0.8
20 Net Leak Rate (1E-8 atm cc/sec)	0.2	0.3	-0.0	0.0	0.7	0.6
21 Measured Dose Rate (1E3 R/hr)	280	44	33	300	58	79
Surface Temperatures (C)						
22 Lid	87	72	70	90	90	87
23 Top Position	120	103	99	125	121	117
24 Second Position	175	140	134	180	159	173
25 Third Position	190	142	140	192	165	179
26 Fourth Position	189	144	135	189	167	182
27 Bottom Position	180	149	123	150	166	172
28 Lower Flange	160	135	105	118	147	151
29 Average of Four	183	144	133	178	164	176
Leak Calculations						
30 Void Pressure (atm)	0.9	1.0	0.9	0.9	1.0	0.9
31 Capsule Pressure (atm)	2.9	2.8	2.7	4.9	2.9	3.1
32 Equivalent Leak Rate (1E-8 atm cc/sec)	0.1	0.2	0.0	0.0	0.5	0.5
Empty Weights						
33 Canister (KG)	73.0	75.1	74.7	72.1	76.4	72.8
34 Lid (KG)	5.1	5.2	5.2	5.2	5.2	5.2
35 Fiberfrax (KG)	0.5	0.5	0.5	0.5	0.5	0.5
36 He Capsule (KG)	0.7	0.7	0.7	0.7	0.7	0.7
37 TOTAL WEIGHT (KG)	79.4	81.5	81.1	78.5	82.8	79.2
Removal						
38 Electropolishing (KG)	1.1	1.1	1.1	1.1	1.1	1.1
39 Full Canister Weight (KG)	234.1	235.9	235.0	225.9	240.4	229.5
40 Glass Mass (KG)	155.8	155.5	155.0	148.5	158.7	151.4
41 Glass Volume (Liters)	59.8	60.2	60.2	63.5	60.9	58.6
42 Approximate Specific Gravity	2.61	2.58	2.57	2.34	2.61	2.58
Smears						
43 Beta + Gamma (d/M/100 cm^2)	LESS THAN DETECTIBLE	LESS THAN DETECTIBLE	LESS THAN DETECTIBLE	LESS THAN DETECTIBLE	LESS THAN DETECTIBLE	LESS THAN DETECTIBLE
44 Alpha (d/M/100 cm^2)	-	-	-	-	-	-
45 Cs-137 Concentration (Ci/Kg)	1236	170	120	1330	240	310
46 Total kCi	193	26	19	198	38	47
47 Sr-90 Concentration (Ci/Kg)	568	940	965	491	1000	1030
48 Total kCi	88	146	150	73	159	156
49 Decay Heat (Watts)	1515	1108	1093	1435	1247	1271

APPENDIX D

VARIANCE ESTIMATES OF CESIUM AND STRONTIUM COMPOSITIONS AND DECAY HEAT

Calculation of the Decay Heat Standard Deviation For an Individual Canister

The total decay heat of a canister is the sum of the decay heats of cesium and strontium. These decay heats are a function of the elements (C_i/Kg) and the volume (liters) and weight (Kg) of the glass in the canister. The formulas for calculating the decay heats of a single canister is as follows.

Decay heat of cesium:

$$DHc = (Mt/Vt)*\left(\sum_{i=1}^{n} V_i*(C_i/209)\right)$$

Decay heat of Strontium:

$$DHs = (Mt/Vt)*\left(\sum_{i=1}^{n} V_i*(S_i/149)\right)$$

Total decay heat:

$$DHT = DHc + DHs = (Mt/Vt)*\left(\sum_{i=1}^{n} V_i*(C_i/209 + S_i/149)\right)$$

where DHc = Decay heat (watts) of cesium in the canister

DHs = Decay heat (watts) of strontium in the canister

DHT = Total decay heat (watts) in the canister

Mt = Total mass (Kg) of glass in the canister

Vt = Total Volume (liters) of glass in the canister

V_i = the volume (liters) of the ith pour

C_i = the cesium of the ith pour in curies per kilogram

S_i = the strontium of the ith pour in curies per kilogram

n = the number of pours.

Conversion of the cesium and strontium from curies per kilogram to watts per kilogram requires dividing by the conversion factors of 209 and 149 respectively. These conversion factors are assumed to be known constants.

The volumes, mass, and the average amounts of cesium and strontium are measured values and are subject to error. These errors are propagated into the overall error of the decay heat measurements. Approximate estimates of the variances of the decay heats are as follows:

$$\mathrm{Var}(DHc) \le ((Mt/Vt)^{**}2)*\left(\sum_{i=1}^{n}(C_i/209)^{**}2\right)*\mathrm{Var}(V_i) +$$

$$(1/Vt^{**}2)*\left(\sum_{i=1}^{n}(V_i*C_i/209)^{**}2\right)*\mathrm{Var}(Mt) +$$

$$((Mt/Vt^{**}2)^{**}2)*\left(\sum_{i=1}^{n}(V_i*C_i/209)^{**}2\right)*\mathrm{Var}(Vt) +$$

$$((Mt/(Vt*209))^{**}2)*\left(\sum_{i=1}^{n}V_i^{**}2\right)*\mathrm{Var}(C)$$

$$\mathrm{Var}(DHs) \le ((Mt/Vt)^{**}2)*\left(\sum_{i=1}^{n}(S_i/149)^{**}2\right)*\mathrm{Var}(V_i) +$$

$$(1/Vt^{**}2)*\left(\sum_{i=1}^{n}(V_i*S_i/149)^{**}2\right)*\mathrm{Var}(Mt) +$$

$$((Mt/Vt^{**}2)^{**}2)*\left(\sum_{i=1}^{n}(V_i*S_i/149)^{**}2\right)*\mathrm{Var}(Vt) +$$

$$((Mt/(Vt*149))^{**}2)*\left(\sum_{i=1}^{n}V_i^{**}2\right)*\mathrm{Var}(S_i)$$

$$\mathrm{Var}(DHT) \le ((Mt/Vt)^{**}2)*\left(\sum_{i=1}^{n}(C_i/209 + S_i/149)^{**}2\right)*\mathrm{Var}(V_i) +$$

$$(1/Vt^{**}2)*\left(\sum_{i=1}^{n}(V_i*(C_i/209 + S_i/149))^{**}2\right)*\mathrm{Var}(Mt) +$$

$$((Mt/Vt^{**}2)^{**}2)*\left(\sum_{i=1}^{n}(V_i*(C_i/209 + S_i/149))^{**}2\right)*\mathrm{Var}(Vt) +$$

$$((Mt/(Vt*209))^{**}2)*\left(\sum_{i=1}^{n}V_i^{**}2\right)*\mathrm{Var}(C) +$$

$$((Mt/(Vt*149))^{**}2)*\left(\sum_{i=1}^{n}V_i^{**}2\right)*\mathrm{Var}(S_i)$$

where Mt = Total mass (Kg) of glass in the canister

Vt = Total Volume (liters) of glass in the canister

V_i = the volume (liters) of the ith pour

C_i = the cesium of the ith pour in curies per kilogram

S_i = the strontium of the ith pour in curies per kilogram

Var(Mt) = the variance of the total mass measurement

Var(Vt) = the variance of the total volume measurement

Var(V_i) = the variance of the ith volume measurement

Var(C) = the variance of the cesium (in Ci/Kg) per pour

Var(S) = the variance of the strontium (in Ci/Kg) per pour

n = the number of pours.

The standard deviations of the decay heats are the square roots of the variances. The variance of the cesium per pour (Var(C)) is calculated from the analytical variance.

$$Var(C) = Var(anal)/na$$

where Var(anal) = the variance of replicate analyses on the same sample from those pours that had multiple analyses

na = the number of replicate analyses per pour.

The variance of the strontium per pour (Var(S)) is similarly calculated by using the strontium data. These estimates of variance do not include the sample-to-sample variability. Therefore they may under-estimate the true variance. The sample-to-sample variance should be small in comparison with the analysis variance (Var(anal)), so the underestimation of the variance should be minimal.

The variances for the mass measure and the volume measures were obtained by assuming a uniform distribution over the tolerance of the measures (1 liter for V_i, 1/3 liter for Vt, and .1% for Mt) and calculating the variance according this distribution. These variance estimates are conservative with respect to the normal distribution and therefore will yield a conservative estimate of the decay heat variance.

The approximate estimates of the variances of the decay heats for each canister depend upon the following assumptions.

1. The correlations between the volume measurements on one canister are either negative or zero. If the correlation is negative, then the above formulas over-estimate the variance. This assumption

should be appropriate especially in the case of two pours per canister since if the volume is measured too high on the first pour, then the volume measured on the next pour will be too low.

2. The variance of the cesium and strontium remains constant from pour to pour.

3. The cesium per pour and the strontium per pour are independent of each other and are independent from pour to pour.

4. The conversion factors are known constants.

Calculation of the Decay Heat Standard Deviation for the Canisters

The estimates of the decay heat standard deviations for the canisters will be approximate not only because of the approximate formula for calculation but also because there were very few replicate analyses done and there were no replicate samples taken. The analytical variance was estimated using the replicate analyses available and was used in the estimate of Var(C) and Var(S).

Table 1 shows the results of the variance estimates along with estimates of the decay heats for each canister. The relative standard deviation (RSD) is the standard deviation divided by the decay heat and multiplied by 100. For example, canister 10 had a total decay heat of 1826.88 with standard deviation 41.68 so the RSD was 2.28 (100 * 41.68 / 1826.88).

TABLE D.1. Decay Heats and Relative Standard Deviations for Each Canister

Canister Number	Glass Mass (Kg)	Glass Volume (Lit.)	Approx. Specif. Gravity	Cs-137 Concent. (Ci)	Cs-137 Decay Heat (Watts)	Cs-137 Std. Dev.	Cs-137 RSD	Sr-90 Concent. (Ci)	Sr-90 Decay Heat (Watts)	Sr-90 Std. Dev.	Sr-90 RSD	Total Decay Heat (Watts)	Total Std. Dev.	Total RSD
1	169.02	60.9	2.78	190112	909.63	16.39	1.80	99664	668.89	33.12	4.95	1578.51	41.20	2.61
2	166.70	59.3	2.81	194248	929.41	15.59	1.68	109417	734.34	43.00	5.86	1663.76	48.54	2.92
3	158.71	59.4	2.67	174986	837.25	13.86	1.66	98805	663.12	36.97	5.58	1500.37	42.13	2.81
5	155.81	59.8	2.61	192559	921.33	14.71	1.60	88467	593.74	36.75	6.19	1515.07	42.13	2.78
6	153.18	59.3	2.58	197602	945.47	14.09	1.49	75058	503.75	49.13	9.75	1449.21	52.09	3.59
7	148.55	63.5	2.34	197572	945.32	14.18	1.50	72972	489.75	34.16	6.98	1435.07	39.06	2.72
8	163.43	59.4	2.75	236974	1133.84	15.93	1.41	87762	589.01	52.48	8.91	1722.85	56.11	3.26
10	159.08	59.8	2.66	182329	872.39	16.15	1.85	142220	954.49	31.56	3.31	1826.88	41.68	2.28
12	171.41	63.1	2.72	197122	943.17	14.61	1.55	77306	518.83	54.90	10.58	1462.00	57.61	3.94
14	156.35	60.6	2.58	189571	907.04	16.30	1.80	70439	472.74	30.16	6.38	1379.78	37.59	2.72
17	157.26	60.6	2.60	177520	849.38	13.96	1.64	66974	449.49	37.96	8.45	1298.87	42.11	3.24
18	159.53	60.2	2.65	197330	944.16	16.92	1.79	143278	961.60	33.79	3.51	1905.76	43.99	2.31
20	158.53	59.8	2.65	193765	927.11	16.49	1.78	141501	949.67	30.39	3.20	1876.77	41.18	2.19
21	153.18	60.2	2.54	186959	894.54	16.00	1.79	90125	604.86	30.39	5.02	1499.41	38.49	2.57
28	165.70	64.2	2.58	169727	812.09	13.46	1.66	130422	875.32	53.50	6.11	1687.41	56.32	3.34
33	143.56	61.8	2.32	55484	265.48	7.31	2.75	146431	982.76	31.81	3.24	1248.23	34.55	2.77
34	163.20	63.6	2.57	136762	654.36	12.55	1.92	146880	985.77	52.91	5.37	1640.13	55.45	3.38
36	162.47	64.2	2.53	73924	353.70	7.08	2.00	158408	1063.14	29.32	2.76	1416.85	32.17	2.27
37	151.41	58.6	2.58	46937	224.58	10.35	4.61	155952	1046.66	49.51	4.73	1271.24	51.08	4.02
38	159.33	59.3	2.69	196582	940.58	17.21	1.83	141714	951.10	33.84	3.56	1891.69	44.24	2.34
41	158.71	60.9	2.61	38090	182.25	10.73	5.89	158710	1065.17	51.73	4.86	1247.42	53.20	4.26
42	155.54	60.2	2.58	26442	126.52	10.44	8.25	146208	981.26	50.60	5.16	1107.77	51.91	4.69
43	154.99	60.2	2.57	18599	88.99	10.36	11.64	149565	1003.79	50.47	5.03	1092.78	51.70	4.73
44	152.27	58.6	2.60	16750	80.14	7.22	9.01	145418	975.96	35.81	3.67	1056.10	36.76	3.48
45	158.62	59.7	2.66	190690	912.39	16.63	1.82	137060	919.86	33.41	3.63	1832.26	43.28	2.36
46	156.80	59.1	2.65	216384	1035.33	14.94	1.44	137984	926.07	50.92	5.50	1961.40	54.95	2.80
47	161.07	59.3	2.72	211807	1013.43	12.89	1.27	126440	848.59	37.36	4.40	1862.02	41.76	2.24
48	164.70	62.9	2.62	233371	1116.61	16.91	1.51	120370	807.85	41.25	5.11	1924.46	47.94	2.49
49	154.27	61.0	2.53	220834	1056.62	16.36	1.55	102923	690.76	39.04	5.65	1747.38	45.39	2.60
50	155.28	59.8	2.60	221374	1059.21	15.79	1.49	105206	706.08	30.24	4.28	1765.29	38.00	2.15

PNL-6790
UC-510

DISTRIBUTION

No. of Copies

OFFSITE

10 DOE/Office of Scientific and Technical Information

4 DOE Office of Civilian Radioactive Waste Management
Forrestal Building
Washington, DC 20585
ATTN: L. H. Barrett, RW-33
S. H. Kale, RW-20
D. E. Shelor, RW-32
R. Stein, RW-23

2 DOE Office of Defense Waste & Transportation Management
GTN
Washington, DC 20545
ATTN: K. A. Chacey, DP-123
T. B. Hindman, DP-12

4 DOE Office of Remedial Action & Waste Technology
GTN
Washington, DC 20545
ATTN: J. E. Baublitz, NE-20
J. A. Coleman, NE-24
T. W. McIntosh, NE-24
H. F. Walter, NE-24

A. T. Clark
Division of Fuel Material Safety
Nuclear Regulatory Commission
Washington, DC 20555

V. Stello
Office for the Executive Director for Operations
Mail Station 6209
Nuclear Regulatory Commission
Washington, DC 20555

No. of Copies

Sheldon Meyers
Environmental Protection Agency
Office of Radiation Programs (ANR-458)
401 M Street S.W.
Washington, DC 20460

J. M. McGough
DOE Albuquerque Operations Office
P.O. Box 5400
Albuquerque, NM 87185

W. McMullen
S. M. Stoller Corp.
3411 Candelaria Rd. N.E.
Albuquerque, NM 87107

E. Maestas
DOE West Valley Project
P.O. Box 191
West Valley, NY 14171

3 DOE Idaho Operations Office
550 Second Street
Idaho Falls, ID 83401
ATTN: C. R. Enos
M. W. Shupe
J. E. Solecki

F. T. Fong
DOE San Francisco Operations
1333 Broadway
Oakland, CA 94612

M. R. Jugan
DOE Oak Ridge Operations Office
P.O. Box E
Oak Ridge, TN 37830

W. T. Goldston
DOE Savannah River Operations Office
P.O. Box A
Aiken, SC 29801

No. of
Copies

M. J. Steindler
Argonne National Laboratory
9700 South Cass Avenue
Argonne, IL 60439

C. S. Abrams
Argonne National Laboratory
P.O. Box 2528
Idaho Falls, ID 83401

3 Battelle Memorial Institute
Project Management Division
505 King Avenue
Columbus, OH 43201
ATTN: W. A. Carbeiner
R. A. Nathan
Technical Library

L. D. Ramspott
Lawrence Livermore National Laboratory
University of California
P.O. Box 808
Livermore, CA 94550

D. T. Oakley, MS 619
Los Alamos National Laboratory
P.O. Box 1663
Los Alamos, NM 87544

4 Oak Ridge National Laboratory
P.O. Box Y
Oak Ridge, TN 37830
ATTN: W. D. Burch
R. T. Jubin
L. J. Mezga
D. W. Turner

2 Sandia Laboratories
P.O. Box 5800
Albuquerque, NM 87185
ATTN: R. W. Lynch
Technical Library

No. of
Copies

J. R. Berreth
Westinghouse Idaho Nuclear Co., Inc.
P.O. Box 4000
Idaho Falls, ID 83401

4 E. I. du Pont de Nemours Company
Savannah River Laboratory
Aiken, SC 29801
ATTN: M. D. Boersma 77341A
J. R. Knight 773A
M. J. Plodinec 773A
C. T. Randall 7042

R. G. Baxter
E. I. du Pont de Nemours Company
Savannah River Plant
Bldg. 704-S
Aiken, SC 29808

A. D. Rodgers
Mail Stop 2411
EG&G Idaho
P.O. Box 1625
Idaho Falls, ID 83415

R. Shaw
Electric Power Research Institute
3412 Hillview Avenue
P.O. Box 10412
Palo Alto, CA 94303

2 West Valley Nuclear Services Company
P.O. Box 191
West Valley, NY 14171
ATTN: J. M. Pope
R. A. Thomas

No. of Copies

ONSITE

J. L. White, Chairman
Energy Research & Development Authority
Empire State Plaza
Albany, NY 12223

6 DOE Richland Operations Office

R. W. Brown
C. E. Collantes
M. J. Furman
R. E. Gerton
P. E. Lamont
E. C. Norman

6 Westinghouse Hanford Company

J. M. Henderson
R. E. Lerch
J. L. Scott
R. A. Smith
D. D. Wodrich
B. A. Wolfe

No. of Copies

30 Pacific Northwest Laboratory

C. R. Allen (3)
R. P. Allen
W. F. Bonner
G. H. Bryan
H. C. Burkholder
C. C. Chapman
T. T. Claudson
M. L. Elliott
R. W. Goles
F. E. Haun
W. O. Heath
L. K. Holton, Jr. (5)
R. F. Klein
J. L. McElroy
R. D. Peters
W. A. Ross
S. C. Slate
J. E. Surma
Publishing Coordination
Technical Report Files (5)